Atmospheric reactivity of biogenic volatile organic compounds in a maritime pine forest during the LANDEX episode 1 field campaign

Kenneth Mermet, Emilie Perraudin, Sébastien Dusanter, Stéphane Sauvage, Thierry Léonardis, Pierre-Marie Flaud, Sandy Bsaibes, Julien Kammer, Vincent Michoud, Aline Gratien, et al.

Science of the Total Environment 756 (2021) 144129

Contents lists available at ScienceDirect

Science of the Total Environment

journal homepage: www.elsevier.com/locate/scitotenv

Atmospheric reactivity of biogenic volatile organic compounds in a maritime pine forest during the LANDEX episode 1 field campaign

Kenneth Mermet [a,b], Emilie Perraudin [a], Sébastien Dusanter [b], Stéphane Sauvage [b], Thierry Léonardis [b], Pierre-Marie Flaud [a], Sandy Bsaibes [c], Julien Kammer [a,c,1], Vincent Michoud [d], Aline Gratien [d], Manuela Cirtog [d], Mohamad Al Ajami [e], François Truong [c], Sébastien Batut [e], Christophe Hecquet [e], Jean-Francois Doussin [d], Coralie Schoemaecker [e], Valérie Gros [c], Nadine Locoge [b], Eric Villenave [a,*]

[a] Univ. Bordeaux, CNRS, EPOC, EPHE, UMR 5805, F-33600 Pessac, France
[b] IMT Lille Douai, Univ. Lille – SAGE, Département Sciences de l'Atmosphère et Génie de l'Environnement, 59000 Lille, France
[c] Laboratoire des Sciences du Climat et de l'Environnement, LSCE, UMR CNRS-CEA-UVSQ, 91191 Gif-sur-Yvette, France
[d] LISA, UMR CNRS 7583, Université Paris-Est Créteil, Université de Paris, Institut Pierre Simon Laplace (IPSL), Créteil, France
[e] Laboratoire Physico Chimie des Processus de Combustion et de l'Atmosphère, PC2A, UMR 8522, 59655 Villeneuve d'Ascq, France

HIGHLIGHTS

- Monoterpenes (MTs) are major contributors to oxidant reactivity in maritime pine forest
- Low abundant BVOCs are usually not considered but some may significantly impact oxidant reactivity budgets
- Results suggest that (β-caryophyllene + O_3) reaction was the main provider of secondary products
- NO_3 was estimated to be unusually maximal during daytime, due to very large MT concentrations and O_3 reactivity at night

GRAPHICAL ABSTRACT

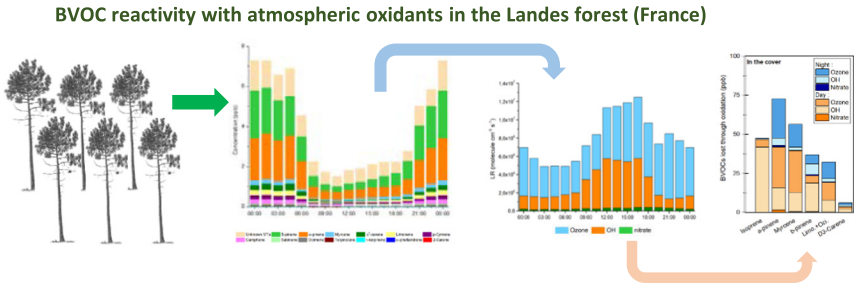

ARTICLE INFO

Article history:
Received 28 May 2020
Received in revised form 18 November 2020
Accepted 21 November 2020
Available online 26 November 2020

Editor: Jianmin Chen

Keywords:
Field campaign
BVOC
Reactivity
Ozone
OH radicals
Nitrate radicals

ABSTRACT

Trace gas measurements were performed during the LANDEX (the LANDes EXperiment) Episode 1 field campaign in the summer 2017, in one of the largest European maritime pine forests (> 95% *Pinus pinaster*) located in southwestern France. Efforts have been focused on obtaining a good speciation of 20 major biogenic volatile organic compounds (BVOCs, including pinenes, carenes, terpinenes, linalool, camphene, etc.). This was made possible by the development of a new and specific chromatographic method. In order to assess the role of BVOCs in the local gas phase chemistry budget, their reactivity with the main atmospheric oxidants (hydroxyl radicals (OH), ozone (O_3) and nitrate radicals (NO_3)) and the corresponding consumption rates were determined. When considering the OH reactivity with BVOCs, isoprene and linalool accounted for 10–47% of the OH depletion during daytime, and monoterpenes for 50–65%, whereas monoterpenes were the main contributors during the night (70–85%). Sesquiterpenes and monoterpenes were the main contributors to the ozone reactivity, especially β-caryophyllene (30–70%), with a maximum contribution during nighttime. Nighttime nitrate reactivity was predominantly due to monoterpenes (i.e. 90–95%). Five specific groups have been proposed to classify the 19 BVOCs measured in the forest, according to their reactivity with atmospheric oxidants and their concentrations. The total amount of BVOCs consumed under and above the forest canopy was evaluated for 7 BVOCs (i.e. isoprene, α-pinene, β-pinene, myrcene, limonene + cis-ocimene and Δ^3-carene). The reactivity of

* Corresponding author.
E-mail address: eric.villenave@u-bordeaux.fr (E. Villenave).
[1] Now at: Department of Chemistry and Environmental Research Institute, University College Cork, Cork, Ireland.

https://doi.org/10.1016/j.scitotenv.2020.144129

atmospheric oxidants and BVOCs at a local level are discussed in order to highlight the compounds (BVOCs, other VOCs), the atmospheric oxidants and the main associated reactive processes observed under the canopy of a maritime pine forest.

1. Introduction

Volatile organic compounds (VOCs) can impact both (i) the air quality and the atmospheric oxidizing capacity (Houweling et al., 1998; Lelieveld et al., 2008; Taraborrelli et al., 2012), due to their reactivity with the main atmospheric oxidants such as ozone (O_3), hydroxyl (OH) and nitrate (NO_3) radicals (Atkinson and Arey, 2003) and (ii) the Earth's radiative budget (Gauss et al., 2006; Hoffmann et al., 1997; Kazil et al., 2010; Stocker et al., 2013), through the formation of ozone and secondary organic aerosols (SOAs).

On global scale, forests are the largest emitters of VOCs covering a wide range of volatility, such as isoprene (C_5H_8), monoterpenes ($C_{10}H_{16}$), sesquiterpenes ($C_{15}H_{24}$) and some oxygenated terpenoids (Kesselmeier and Staudt, 1999). Each of these groups of compounds exhibits a large number of structural isomers, with a large range of reactivity.

The impact of biogenic VOC (BVOC) emissions on the carbon cycle and the atmospheric oxidant budget at both local and global scales is currently not well understood. Indeed, reported measurements of total OH reactivity performed in ambient air highlighted some gaps in our knowledge about OH sinks, where the measured OH reactivity is frequently higher than that calculated from concomitant VOC observations (Di Carlo et al., 2004; Dusanter and Stevens, 2017; Edwards et al., 2013; Griffith et al., 2013; Hansen et al., 2014; Hens et al., 2014; Wolfe et al., 2014; Zannoni et al., 2017 and references therein). This difference reveals the presence of unmeasured OH sinks within the forest boundary layer, which may either be attributed to unidentified primary BVOC emissions (Di Carlo et al., 2004; Sinha et al., 2010), or to BVOC oxidation products (Edwards et al., 2013; Hansen et al., 2014; Lou et al., 2010; Mao et al., 2012; Zannoni et al., 2017) or both (Nölscher et al., 2012). A recent study using the Positive Matrix Factorization (PMF) approach to characterize the sources of particulate components over forests demonstrated the important impact of BVOC oxidation products on aerosol composition (Freney et al., 2018). Extensive molecular analyses of SOA have only partially been performed yet (Plewka et al., 2006; Capes et al., 2009; Gómez-González et al., 2012; Kourtchev et al., 2016; Freney et al., 2018) to better understand the link between SOA and primary BVOCs. The speciation of BVOCs in forest environments, their in-situ reactivity and the consecutive formation of SOA, are therefore important aspects that need to be further investigated to improve our understanding on atmospheric processes.

Several studies have recently described the reactivity of BVOCs with the three main atmospheric oxidants in specific forests and their capacity to form VOC oxidation products (Hellén et al., 2018; Yáñez-Serrano et al., 2018). They demonstrated that the most abundant compounds do not automatically imply the highest reactivity, and therefore that they may not be the most atmospheric relevant compounds. In addition, these authors showed that the relative contribution of the different VOCs to the oxidative budget may change over time. Hellén et al. (2018) particularly demonstrated that β-caryophyllene, despite its low levels of concentration, was an important contributor to the formation of BVOC oxidation products in the Finnish boreal forest, and that ozonolysis was the dominant reactive process for BVOCs, during both night and day.

The Landes forest is one of the largest European forests, covering an area of about 1 million hectares in southwestern France. A previous study from our group, LANDEX (The Landes Experiment) Episode 0 project in July 2015, reported the first observations of BVOC reactivity in this forest, in relation to nighttime biogenic new particle formation (NPF) (Kammer et al., 2018). It was suggested that monoterpene oxidation may contribute to these NPF events, especially through ozonolysis processes.

This study is part of the LANDEX Episode 1 project, involving 12 different partners. Its objective was to improve our understanding of physical and chemical processes governing the formation and growth of SOAs from biogenic origin at a specific forested site. Among other actions, a specific effort was carried out to obtain a good speciation of 20 major BVOCs (including pinenes, carenes, terpinene, linalool, camphene, etc.), which was possible thanks to the development of a new chromatographic method (Mermet et al., 2019). In order to assess the role of BVOCs in the gas phase chemistry budget, their reactivity with the main atmospheric oxidants (OH, O_3 and NO_3) and the corresponding consumption or production rates of primary and secondary compounds, respectively, were quantified. The reactivity of atmospheric oxidants and BVOCs at a local scale is discussed in order to highlight the key compounds (BVOCs, other VOCs), the atmospheric oxidants and the main associated reactive processes observed under the canopy of a maritime pine forest.

2. Materials and methods

2.1. Site description

The measurements were conducted as part of the LANDEX Episode 1 field campaign from June 29th to July 20th 2017. The measurement site was located at Bilos (Salles) in the French Landes Forest (44°29′39.69″N, 0°57′21.75″W, and 37 m above sea level). A short description of the site, which is also part of the European ICOS Ecosystem infrastructure (Integrated Carbon Observation System, www.icos-cp.eu/observations/ecosystem/stations), is presented in Fig. S1 and more details can be found elsewhere (Moreaux et al., 2011; Kammer et al., 2018). Briefly, the site is a plot of maritime pines (*Pinus pinaster* Aiton) of 30.2 ha (570 × 530 m). The understorey was dense and composed of gorse (*Ulex europaeus* L.), grass (*Molinia caerulea* (L.) Moench) and heather (*Calluna vulgaris* (L.) Hull). Tree height was approximately 10 m, in summer 2017. The soil is a sandy acidic hydromorphic podzol with a discontinuous layer of iron hard pan at a 75 cm depth. The climate is locally temperate, with a maritime influence due to the proximity of the North Atlantic Ocean (ca. 25 km westbound).

2.2. Instruments

A detailed description of the location of all instruments on the measurement site is presented in Bsaibes et al. (2020). Meteorological parameters were measured on a mast during the campaign, at 15 m above ground level (a. g. l.). Air temperature and relative humidity (HMP 155, VAISALA HUMICAP), wind speed and direction (Windsonic 1, Campbell scientific), global solar radiation (CMP22 and CNR4, Campbell scientific) and rainfalls were continuously measured at a half hourly scale. A 3D sonic anemometer (R3, Gill instruments) localized at the top of the mast allowed to characterize the turbulence. Friction velocity was measured thanks to the Eddy-covariance technique. Mixing layer height measurements were performed using a ceilometer (VAISALA CL31).

The mobile laboratory truck from EPOC was deployed and located between two ranks of trees. The measurement height was adjusted at 6 m above ground level (a. g. l.), below the forest canopy. The gaseous sampling was performed through a 5-m long Teflon tubing (4.5 mm inner diameter). Ozone and nitrogen oxides ($NO_x = NO + NO_2$) were

monitored through a UV absorption analyzer (APOA 370, HORIBA, detection limit (DL) = 0.5 ppb) and a chemiluminescence analyzer (APNA 370, HORIBA, DL = 0.5 ppb), respectively. Both monitors were calibrated before the campaign, and instrument background checks were frequently performed using activated charcoal air filters. Note that a Cavity Attenuated Phase Shift (CAPS) technique was deployed by the LISA partner to provide an extremely sensitive, fast and accurate NO_2 concentration measurement but, unfortunately, it did not work properly during the campaign.

The mobile laboratory from IMT Lille Douai (IMTLD) was deployed on the same rank of trees. Two gas chromatographic instruments (GC) were used, one to monitor 20 C_5-C_{15} BVOCs (called GC-BVOC1, Mermet et al., 2019), including isoprene, α- and β-pinene, carenes, α- and γ-terpinene, linalool, camphene, etc., at 6 m height a.g.l. and the second one to monitor 65 C_2-C_{14} non-methane hydrocarbons (NMHC), including alkanes, alkenes, alkynes and aromatics (see the full list in Table S1 – 1) at 12.5 m height a.g.l. (called GC-NMHC). Both GC were run at a time resolution of 90 min. GC-BVOC1 consisted of an online thermodesorber system (Markes Unity 1) coupled to a GC system (6890 N, Agilent) and a flame ionization detector (FID). Ambient air was sampled at a flow rate of 20 mL/min for 60 min through a trap filled with Carbotrap B held at 20 °C by a Peltier-cooler system. The sample was thermodesorbed at 325 °C and injected into a BPX5 column (60 m × 0.25 mm × 1 μm) using helium as carrier gas. For further details, refer to Mermet et al. (2019). The sampling was done through a 10 m long sulfinert heated (55 °C) tube (1/4″) continuously flushed at 1 L/min with an external pump. The sampling line was equipped with an ozone scrubber (Copper tube impregnated with KI) and a particle filter. A certified standard containing a mixture of 33 VOCs (Table S1-2) at a concentration level of 4 ppb (NPL Teddington UK, 2014) was used for calibration at the beginning, middle and end of the campaign. GC-NMHC was an online GC system with two columns and two FID detectors. This instrument has been previously described in detail elsewhere (Badol et al., 2004). Ambient air was sampled through a 13-m long sulfinert heated (55 °C) tube (1/4″), equipped of an ozone scrubber (copper tube impregnated of KI) and a particle filter, at a flow rate of 2 L/min using an external pump. The instrument sampled from this line at a flow rate of 15 mL/min. The air sample was first dried using a Nafion membrane and subsequently passed through a sorbent trap containing Carbotrap B and Carbosieve S III at −30 °C (Peltier cooling system) for 40 min. The sample was thermodesorbed at 300 °C and introduced into the GC system. A switch was used to feed the two capillary columns, the first column being designed for C_6-C_{14} compound separation (CP-Sil 5 CB, 50 m × 0.25 mm × 1 μm) and the second for C_2-C_5 compound separation (plot Al_2O_3/Na_2SO_4, 50 m × 0.32 mm × 5 μm). Helium was used as carrier gas. A certified standard containing a mixture of 30 VOCs at a concentration level of 4 ppb (NPL, Teddington, UK, 2016) was used for calibration at the beginning, middle and end of the campaign.

A third mobile facility, located between two other ranks of trees (next to the other facilities), was housing a proton transfer reaction-mass spectrometer (PTR-MS) and a GC system (GC-BVOC2) to characterize VOCs. The PTR-MS set-up was recently described by Bsaibes et al. (2020). Briefly, the PTR-MS (PTR-QiToF-MS, Ionicon) and the ozone analyzer were connected to a high flow rate sampling system allowing sequential measurements at 4 different levels (L1 = 12 m, L2 = 10 m, L3 = 8 m, L4 = 6 m) with a cycling time of 30 min (6 min at each level and 6 min of zero air). This system was composed of four identical heated (55 °C) sampling lines (PFA, 1/4" OD) of 15 m, Teflon solenoids valves and an external pump. The lines were constantly flushed at 10 L/min. Teflon (PFA) particle filters were added at the inlet. The PTR-MS sampled air from the high flow rate system through a 1.5-m long heated (60 °C) inlet (PEEK, 1/16" OD) at a flow rate of 300 mL/min. The drift tube was operated at a pressure of 3.8 mbar, a temperature of 70 °C and a E/N ratio of 131 Td. Calibrations of ion transmission were performed every 3 days using the Gas Calibration Unit (GCU, Ionicon) and a certified gas mixture provided by Ionicon (15 compounds at approximately 1 ppm, including methanol, acetaldehyde, acetone, aromatic compounds, chlorobenzenes, etc.). Measurements of methacrolein + methylvinylketone + ISOPOOH (isoprene hydroxyl hydroperoxides) fragment, the sum of monoterpenes, the sum of sesquiterpenes, nopinone and pinonaldehyde from levels 1 and 4, corresponding to the levels where the GC measurements were performed, are discussed in this work. No correction was applied to account for the fragmentation of sesquiterpene, nopinone and pinonaldehyde in the drift tube. A second UV absorption analyzer (O342e, Environnement SA) was also deployed to measure ozone and was connected to the high flow rate sampling system of the PTR-MS.

A speciation of C_6-C_{12} VOCs has been performed using a GC-FID (airmoVOC C_6-C_{12}, Chromatotec) at the 12-m height a.g.l. with a time resolution of 30 min. The ambient air was sampled through a sorbent trap containing Carbopack C at room temperature and a flow rate of 60 mL/min for 10 min. The sample was thermodesorbed at 380 °C and injected into a MXTE30CE column (30 m × 0.28 mm × 1 μm), with dihydrogen as carrier gas. Further details can be found elsewhere (Gros et al., 2011). The sampling was performed using a 13 m long sulfinert heated line (55 °C, 1/8″) connected to an external pump for continuous flushing. An ozone scrubber (Copper tube impregnated with KI) and a particle filter were added to the inlet. A certified standard mixture containing 16 VOCs (including 8 terpenes) at a concentration level of 2 ppb (NPL, Teddington UK, 2014) was used for calibration at the beginning, middle and end of the campaign. For all GCs, a mean response factor was used for each VOC for the whole campaign as the reproducibility between the 3 calibrations was better than 5% for all VOCs. Note that other laboratory facilities specifically related to this work were deployed during the campaign, particularly to measure atmospheric oxidants such as NO_3 (IBBCEAS technique from the LISA laboratory – University Paris-Est Creteil) and OH (FAGE technique from the PC2A laboratory- University of Lille (Amedro et al., 2012)). Because of technical problems (FAGE) and radical measurements being below the detection limit (IBBCEAS), the choice was made not to present the partial evolution of this data in this work. However, the methodology allowing to access to concentration proxies of these species is proposed in Section 3.4.

2.3. Calculation of oxidant consumption rates

The total reactivity of VOCs (R_x) with an atmospheric oxidant x (i.e. OH, NO_3 or O_3) was calculated by combining their respective concentrations [VOC_i] with the corresponding reaction rate constants ($k_{i,x}$):

$$R_x = \sum [VOC_i] k_{i,x} \quad (1)$$

An analysis based on Eq. (1) allows assessing the contribution of the different VOCs (or class of VOCs) to the total loss rate of either OH, NO_3 or O_3. A list of reaction rate constants used in this work is available in the Supplementary Information section (Table S1).

For "unknown" monoterpenes (MTs), i.e. not identified or measured by GC, their concentration was evaluated as the difference between the sum of monoterpenes measured by chromatography (GC-BVOCs) and by PTR-MS. For "unknown" sesquiterpenes (SQTs), their concentration was determined as the difference between the β-caryophyllene concentration measured by GC-BVOCs and the sum of SQTs measured by PTR-MS.

For unknown SQTs and MTs, the reaction rate constants were taken as the medians of the reported rate constants (at room temperature) for SQT or MT (listed in Table S1): For MT: $k_{OH} = 1.17 \times 10^{-10}$ cm^3 molecule^{-1} s^{-1}, $k_{O3} = 1.50 \times 10^{-16}$ cm^3 molecule^{-1} s^{-1}, $k_{NO3} = 1.10 \times 10^{-11}$ cm^3 molecule^{-1} s^{-1}; for SQT: $k_{OH} = 2.00 \times 10^{-10}$ cm^3 molecule^{-1} s^{-1}, $k_{O3} = 3.55 \times 10^{-16}$ cm^3 molecule^{-1} s^{-1}, $k_{NO3} = 8.20 \times 10^{-12}$ cm^3 molecule^{-1} s^{-1}).

The total OH reactivity measured during the intensive LANDEX field campaign has already been reported by Bsaibes et al. (2020) and compared with a calculated OH reactivity, using a weighted rate constants for all monoterpenes, to estimate its missing part. BVOCs, i.e. isoprene and (non-oxygenated and oxygenated) monoterpenes, were found to be the main contributors to the calculated total OH loss rate, with average contributions of 18% and 75%, respectively. Here, the approach is different: the aim was to identify the individual contribution of each BVOC to the total BVOC reactivity and the main losses for each BVOC. In the case of ozone, the total reactivity was calculated considering only reactions with BVOCs and with NO. Reactions with other VOCs were not presented here as their total contribution represented less than 1% of the calculated total ozone reactivity. The same approach was used for the total nitrate radical reactivity.

NO concentrations were mostly below the limit of detection of 0.5 ppbv. It is assumed that air masses above were decoupled from air masses inside the canopy. So, an upper limit could be calculated considering that ozone depletion rate during night was caused only by oxidation reactions with unsaturated BVOCs and with NO (Eq. (2)). The highest value obtained (140 ppt) was used when NO concentration measured were below the limit of detection.

$$[NO] = \frac{1}{k_{NO+O_3} \times [O_3]} \left[\frac{d[O_3]}{dt}_{max} - [O_3]\tau_{O_3\ without\ NO} \right], \quad (2)$$

where $\frac{d[O_3]}{dt}_{max}$ is the maximum depletion rate obtained for a dt of 90 min, and $\tau_{O3\ without\ NO}$ is O_3 lifetime without NO.

The lifetime of ozone was calculated considering oxidation reaction with unsaturated BVOCs:

$$\begin{aligned}(\tau_{O_3\ without\ NO})^{-1} = &\sum k_{O_3+MT_i}[MT_i] + k_{O_3+isop.}[isop.] \\ &+ k_{O_3+\beta-caryo.}[\beta-caryophyllene] \\ &+ k_{O_3+"unknown"SQT}["Unknown"SQT] \end{aligned} \quad (3)$$

2.4. Calculation of the oxidant contribution to the consumption rates of BVOCs

The contribution of each atmospheric oxidant (f_{Ox}) to the total reactivity of a specific VOC was calculated as:

$$f_{Ox} = \frac{k_{Ox_i}[Ox_i]}{\sum_{Ox_i} k_{Ox_i}[Ox_i]}, \quad (4)$$

where [*Ox*] is the concentration of an oxidant, either OH, NO_3 or O_3, and k_{Ox} the rate constant of the reaction between this oxidant and the targeted VOC.

Due to technical problems with the FAGE instrument along the campaign with only short measurement periods, the OH radical concentration was estimated considering (i) a stationary value during the night, evaluated at 1×10^5 molecule cm^{-3}, and (ii) a proxy of the concentration during the day accounting for the change in solar radiation. The model was defined as follows:

$$[OH]_t = 1 \times 10^5 + \frac{Glob.Rad_t \times K_{a,t}}{943.54} \times \left[[OH]_{max} - 1 \times 10^5 \right], \quad (5)$$

where: 1×10^5 molecule cm^{-3} is a concentration regularly observed during the night in forested environments (Berresheim et al., 2000; Birmili et al., 2003; Petäjä et al., 2009; Griffith et al., 2013; Hens et al., 2014); $Glob.Rad_t$ (W m^{-2}) is the solar radiation intensity measured at time t above the canopy; 943.54 W.m^{-2} is the maximum of the radiation intensity obtained for clear sky conditions during the campaign above the canopy; $K_{a,t}$ is a canopy time-dependent transmission coefficient to calculate [OH] below the canopy. It has been calculated considering the campaign mean diurnal ratio between the solar radiation intensity measurements above and below the canopy at a resolution time of 30 min and averaged over 90 min to correspond to the sampling time of GC-FID instruments. Two $[OH]_{max}$ values were used to define upper and lower limits of ambient OH. From Bsaibes et al. (2020), the OH concentration was equal to 4.2×10^6 molecule cm^{-3} on average during daytime, with a maximum of 4.3×10^7 molecule cm^{-3}, and around 1.5×10^6 molecule cm^{-3} on average during nighttime (for the 13th to 19th July period). However, they reported a potential artifact on OH radical measurements, leading to a possible overestimation of OH radical concentrations. Therefore, for the upper limit, $[OH]_{max}$ was selected to be equal to 6×10^6 molecules cm^{-3} as measured by Birmili et al. (2003), while for the lower limit $[OH]_{max}$ was set at 3×10^6 molecules cm^{-3}, as reported by Hens et al. (2014).

Nitrate radical measurements were systematically lower than the detection limit of the IBBCEAS instrument during the campaign (3–5 ppt for a time resolution of 1 min) which was sampling at 4.5 m a.g.l. Therefore, the nitrate concentrations under the canopy were calculated assuming steady state between its production rate from $O_3 + NO_2$ reaction and its destruction rate from photolysis and its reactions with BVOCs as described by Peräkylä et al. (2014):

$$[NO_3]_{steady-state} = F_{NO_3}\tau_{NO_3}, \quad (6)$$

where $F_{NO3}$is the production rate of NO_3 (in molecule cm^{-3} s^{-1}) and τ_{NO3} its lifetime (in s). The NO_3 production rate was calculated from the following equation:

$$F_{NO_3} = k_{O_3+NO_2}[O_3][NO_2], \quad (7)$$

The temperature - dependent expression was used to calculate the reaction rate constant $k_{O3+NO2} = 1.4 \times 10^{-13}$ exp.$(-2470/T)$ cm^3 molecule^{-1} s^{-1} (Vrekoussis et al., 2004) with T in Kelvin. An upper limit of the NO_3 lifetime was calculated considering photolysis processes and its main reactions, according to:

$$\begin{aligned}(\tau_{NO_3})^{-1} = &J(NO + O_2) + J(NO_2 + O) + \sum (k_{NO_3+MT_i}[MT_i]) \\ &+ k_{NO_3+NO}[NO] + k_{NO_3+isop.}[isoprene] \\ &+ k_{NO_3+\beta-caryophyllene}[\beta-caryophyllene] \\ &+ k_{NO_3+SQT_{Un.}}[SQT_{Un.}] \end{aligned} \quad (8)$$

A fast CCD spectroradiometer, running at a time resolution of 10 s, measured $J(NO_3)$ only between the 12th to the 19th July. Therefore, linear models were used to obtain $J(NO_3)$ for the whole campaign. The global irradiance measured on site was found to be a good proxy to model the photolysis rates according to:

$$J(NO + O_2) = 1.6 \times 10^{-4} \times Glob.Rad_i, \quad (9)$$

and

$$J(NO_2 + O) = 2.0 \times 10^{-5} \times Glob.Rad_i, \quad (10)$$

These linear models were compared to the measurements from the spectroradiometer. The differences between calculated (Eqs. (9) and (10)) and measured $J(NO_3)$ values were lower than 30% between 9:30 am and 6:00 pm UTC.

Note that these calculations do not take into account the equilibrium with N_2O_5 and especially heterogeneous reaction of N_2O_5 which have a major impact on the NO_3 radical budget especially under high RH.

Above the canopy, Eq. (8) was used to calculate NO_3 concentration, with MT concentrations measured by GC-BVOC2 and sesquiterpenes and unknown monoterpene concentrations obtained by PTR-MS at 12 m a.g.l. The reaction rate constants used for all identified compounds are reported in Table S2. For unknown monoterpenes and sesquiterpenes, the same reaction rate constants as detailed in Section 2.3 were used.

As specified above, the reaction rate constants and the concentrations used in Eq. (8) were detailed for each BVOC (Table S2) and

measured in the forest canopy by the different GC-BVOCs. Above the canopy, monoterpene and sesquiterpene concentrations were measured by PTR-MS. The reaction rate constant used for monoterpenes was the mean of all monoterpene reaction rate constants weighted by the individual concentration ratio of each compound to the total monoterpenes measured by the GC-BVOC2. For sesquiterpenes, the reaction rate constant used in the calculations was the same as that evaluated for unknown sesquiterpenes. Finally, isoprene concentration was provided by the GC-NMHC.

A full sensitivity test was performed with each terms of the calculation formula of NO_3 concentrations, applying a complete error propagation study, according to Taylor and Kuyatt (1994) (NIST Technical Note 1297 - Guidelines for evaluating and expressing the uncertainty of NIST measurement results):

$$u^2(y) = \sum_{i=1}^{n}\left[\frac{\partial f}{\partial x_i}\right]^2 * u2(x_i) + 2\sum_{i=1}^{n-1}\sum_{j=i+1}^{n}\frac{\partial f}{\partial x_i}\frac{\partial f}{\partial x_j}u(x_i)\,u(x_i)r(x_i,x_j) \quad (11)$$

where *u* represents the global uncertainty of the measured variable under consideration, *f* the function used to calculate the target term, *xi* and *xj* two variables and *r* the correlation coefficient between these two variables *xi* and *xj*.

The considered variables were O_3, NO_2, NO and all VOC concentrations, and J and k constants. Varying concentrations of O_3 by 3% (2 ozone analyzers on site and ozone measurements by ICOS), of NO_2 by 60%, of NO by 200% (because very close to the DL), of BVOCs from 5% (for α-pinene) to 100% (for 2-carene) with 70% for β-caryophyllene for instance, $J(NO_3)$ by 60% and all second order rate constants of (BVOC + NO_3) reactions by 25% leads to an overall uncertainty of 110% on NO_3 global concentrations.

Considering all uncertainties related to the calculation of NO_3 concentration profile, despite the appropriated approach used, NO_3 values were systematically multiplied and divided by 2 in the analysis to assess a reasonable uncertainty on the importance of NO_3 reactions to the total BVOC loss in the forest.

2.5. Calculation of the VOC loss rate

The consumption rate of a specific VOC (LR_{VOC}) was calculated according to Eq. (11):

$$LR_{VOC} = [VOC]\left(k_{OH}[OH] + k_{O_3}[O_3] + k_{NO_3}[NO_3]\right), \quad (12)$$

where k_{OH}, k_{NO3} and k_{O3} are the rate constants (in cm^3 $molecule^{-1}$ s^{-1}) for the reactions of the targeted VOC with OH, NO_3 and O_3, respectively.

The amount of BVOC consumed during the whole field campaign was calculated as the sum of each half-hourly calculated LR_{VOC} (all measured BVOCs) multiplied by the time resolution of the VOC measurements used in Eq. (11) (i.e. 5400 s at the 6-m height and 1800 s at 12-m height). These calculations were performed for the period from the 30th of June at 19:30 UTC to the 13th of July at 10:00 UTC.

3. Results and discussion

3.1. Evolution of physico-chemical parameters and gaseous phase composition

During the intensive field campaign, the meteorological conditions were most of the time significantly different from those reported for the last 10 years in this region in summer (Fig. 1). Large cloudy passages

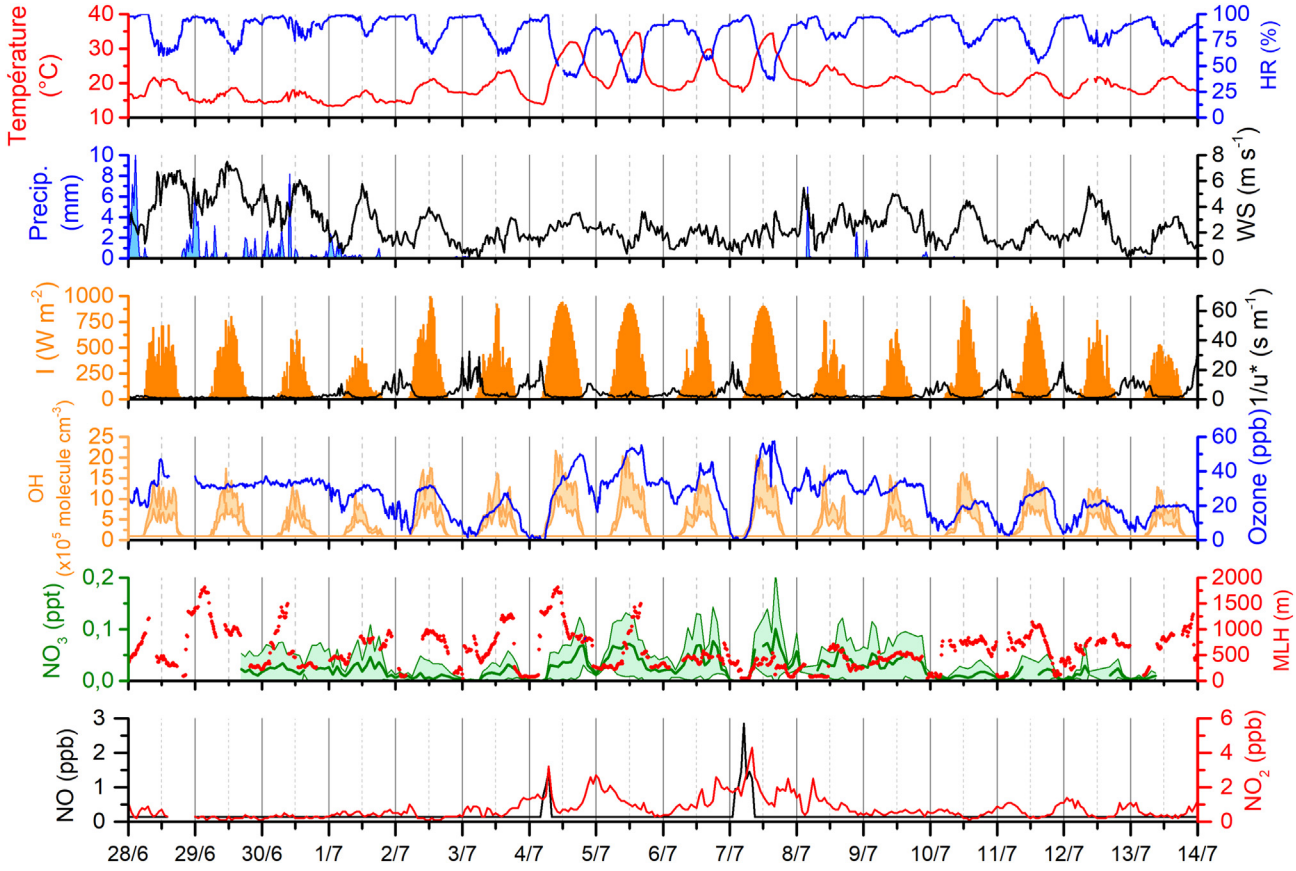

Fig. 1. Time series of meteorological parameters, NOx, main atmospheric oxidant concentrations (calculated OH, high and low concentration scenarios, measured O_3 and calculated NO_3 with the associated uncertainties (k = 2, envelopes)) at 6 m a.g.l. (under the canopy) during the LANDEX Episode 1 campaign. I: Irradiance; WS: wind speed at 6 m, RH: relative humidity. MLH: Mixing Layer Height.

or regular rainfall events occurred between June 28th and July 3rd and also in the July 8th to July 13th 2017 period. These two precipitation periods were associated with low solar radiation (< 750 W m^{-2}), mild summer temperatures (< 25 °C), high relative humidity ($> 75\%$) and moderate winds. These periods, not favourable to atmospheric photooxidation, were therefore defined in this work as "low oxidation" periods. On the other hand, two episodes of sunny conditions were observed during the campaign, i.e. from July the 4th to the 7th then from the 14th to the 18th. These periods were characterized by elevated temperatures with daily maxima above 25 °C, relative humidity below 50% (during the day), low wind speeds (< 3 m s^{-1}) and no precipitation. These periods, favourable to plant emissions and strong oxidant formation, were defined below as periods of "strong oxidation".

As detailed above, monoterpenes were monitored using 3 different instruments, i.e. 2 GC instruments and one PTR-MS, at two different heights (6 m (Fig. 2) and 12 m (Fig. S2)). The PTR-MS measured the total concentration of all monoterpenes at *m/z* values of 137 (i.e. their main fragment) and 81 (their second most important fragment), with the exception of p-cymene at m/z 135. As it can be seen on Figs. 2 and S3, the concentrations of monoterpenes determined by GC and PTR-MS were in good agreement. At the 6-m height, the 12 non-oxygenated monoterpenes (α-pinene, β-pinene, myrcene, Δ^3-carene, sabinene, terpinolene, camphene, limonene, ocimene, γ-terpinene, 2-carene and α-phellandrene) measured by GC accounted for 80% of the total monoterpene concentration measured by PTR-MS. At the 12-m height, only 6 monoterpenes (α-pinene, β-pinene, myrcene, Δ^3-carene and limonene + cis-ocimene) were measured, contributing to 63% of the PTR-MS measurements.

To simplify the presentation of the results, the term monoterpenes (or MTs) will correspond to monoterpene measurements by PTR-MS, which does not include oxygenated monoterpenes. Monoterpenes (with mean concentrations of (3.91 ± 4.71) ppb) were the most abundant terpenoids observed on site with maximal concentrations observed during the night, i.e. between 22:00 and 4:00 UTC at both heights (Figs. 2 and S2). β- and α-pinene were the most abundant monoterpenes measured (presenting mean concentrations of (1.17 ± 1.69) ppb and (1.15 ± 1.47) ppb, respectively) at Bilos site, their sum representing around half of the total monoterpene concentration at both heights.

Emissions of β- (1.7 ppb mean concentration) and α-pinene (1.3 ppb), Δ^3-carene (0.6 ppb), limonene+1,8-cineole (1.1 ppb) and camphene (0.3 ppb) were previously reported by Simon et al. (1994) in 1992 in the Landes forest, for 13 m height pine trees. Very recently, Kammer et al. (2020) measured at Bilos monoterpene mixing ratios frequently reaching about 15 ppb in 2015, whereas they were always lower than 10 ppb in 2014. Finally, Li et al. (2020b) measured at the same site but in 2018, mean values for monoterpene mixing ratio of 6 ppb, with maxima up to 41.2 ppb, due to very favourable (high ambient temperatures and very sunny) meteorological conditions.

Diurnal variation of monoterpene concentrations was mostly dependent on the vertical atmospheric turbulence, the inverse of the friction velocity u* (1/u* in s m^{-1}) being used here to represent atmospheric stability. A strong vertical concentration gradient was observed more particularly during nighttime when 1/u* was above 5 s m^{-1} (corresponding to the nights of the 4th to the 7th of July included and the nights of the 9th to the 17th of July), the concentrations being lower above the canopy due to a stratification of the vertical mixing layer. This stratification was confirmed by the mixing layer height measurements (Fig. 1). Monoterpene concentration maxima were also partly explained by the temperature of the day before the night, in accordance with a temperature-dependent emission, as already reported for monoterpenes in the literature (Laothawornkitkul et al., 2009; Niinemets et al., 2010). Similar diurnal variations were observed for monoterpenes in a Scots pine forest (Petersson, 1988), in a boreal forest (Hellén et al.,

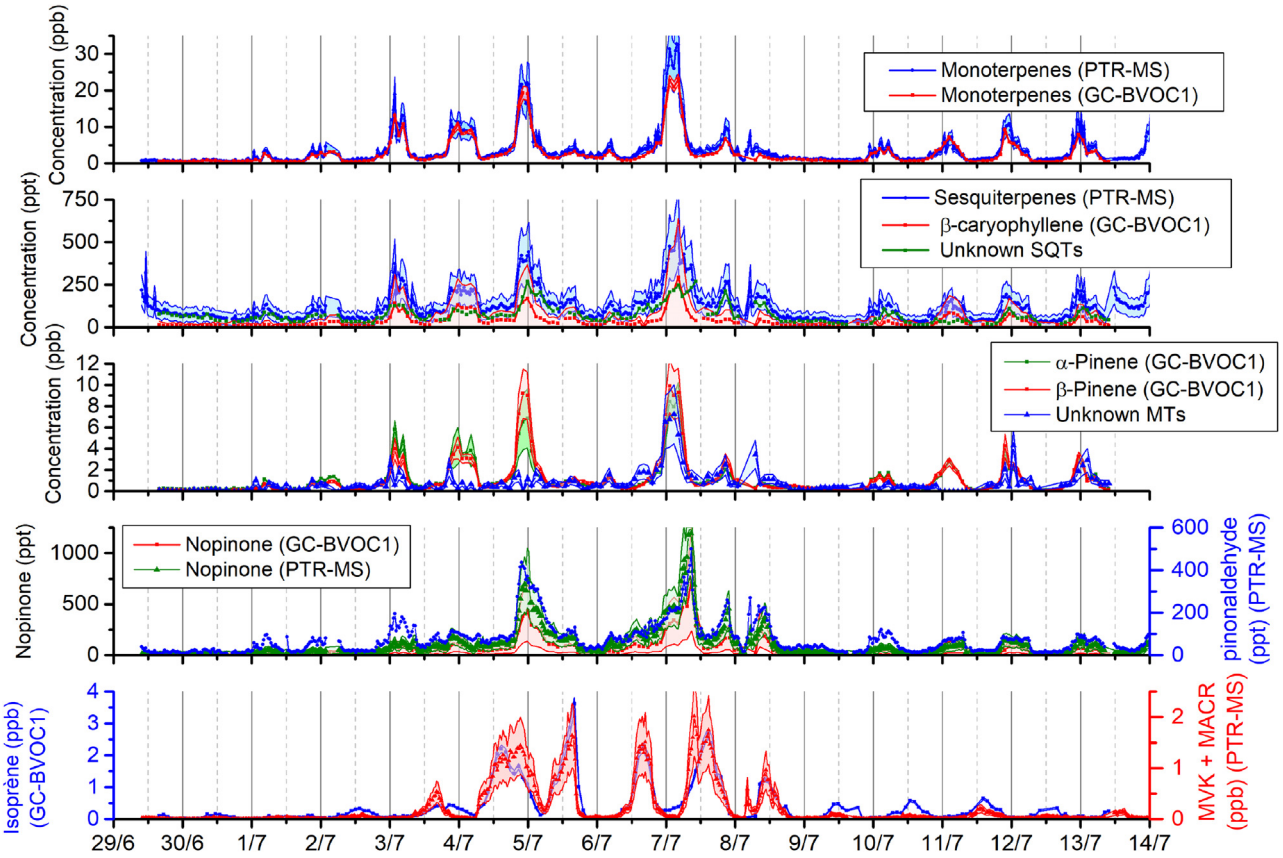

Fig. 2. Time series of BVOC concentrations with their associated uncertainties (k = 2, envelopes) measured at 6 m a.g.l. (under the canopy) during the LANDEX Ep.1 field campaign. Compounds measured by the GC-BVOC1.

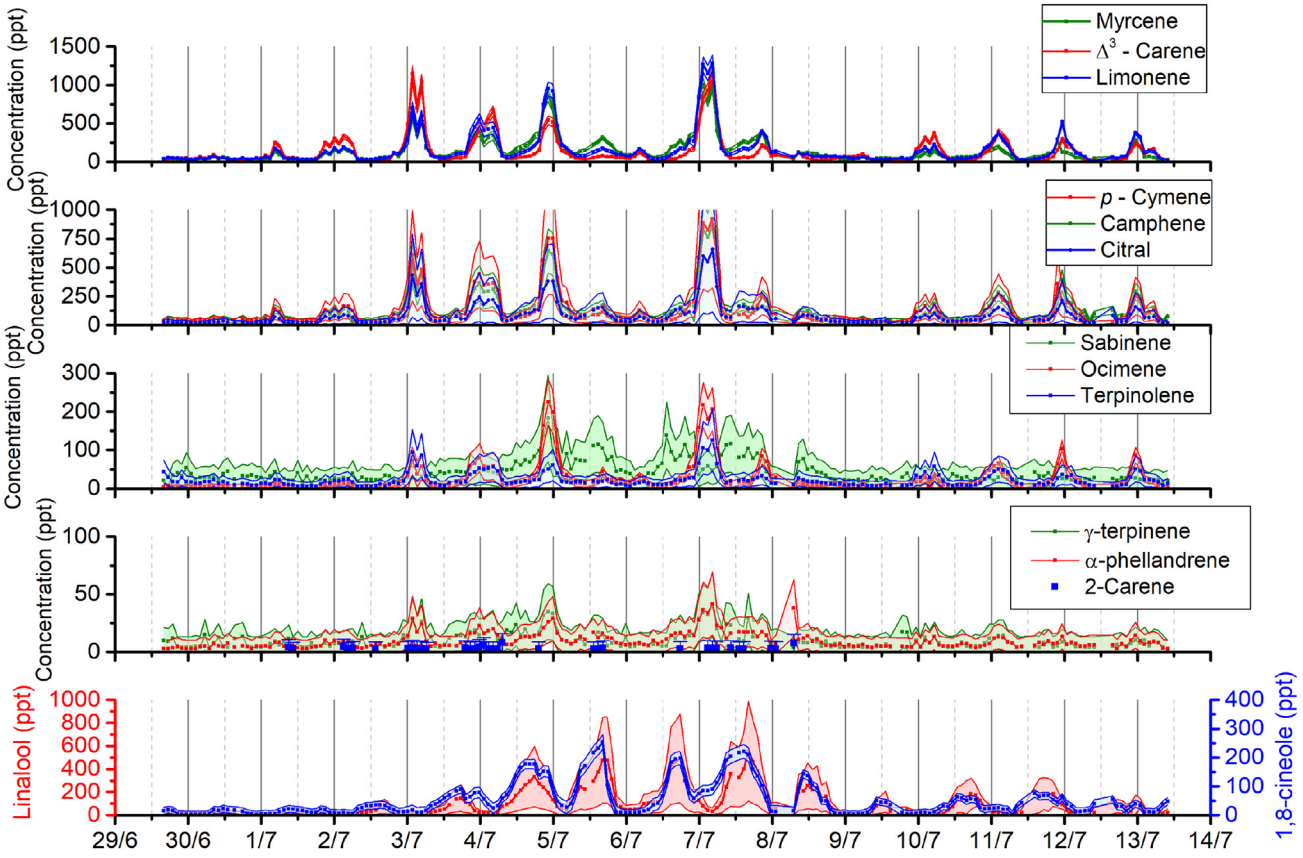

Fig. 2 (*continued*).

2018), in the Blodgett Forest in California (Bouvier-Brown et al., 2009), in a ponderosa pine forest (Kaser et al., 2013) or in a deciduous evergreen forest (Kaiser et al., 2016), and in the Amazonian forest (Yáñez-Serrano et al., 2018). Monoterpene concentrations reported by Petersson (1988) were comparable to those measured in the Landes forest, reaching up to (11–19) ppb at maximum. For the other sites, they were lower in average: 0.7 ppbv, Hellén et al., 2018; 1.5 ppb (Bouvier-Brown et al., 2009), (1.03 ± 0.09) ppb (Kaser et al., 2013), around 1 ppb (Kaiser et al., 2016) and around 0.7 ppb at 12 m and 0.6 ppb at 24 m (Yáñez-Serrano et al., 2018).

Calculated OH concentrations within the canopy over the campaign are presented in Fig. 1. Daily maxima ranged from 1×10^6 to 2.2×10^6 molecules cm^{-3} and from 5×10^5 to 1.2×10^6 molecules cm^{-3} and daily averages were equal to 8×10^5 and 4.4×10^5 molecules cm^{-3}, for the upper and lower limits respectively.

NO_x concentrations were low during the campaign (i.e. (1.1 ± 1 0.1) ppb on average), well-corresponding to low- or non-anthropized site. NO concentrations were mostly under the detection limit (0.5 ppb), while NO_2 concentrations values were about (0.82 ± 0.62) ppb. As NO_X were monitored using a chemiluminescence analyzer (with a molybdenum converter), being subject to positive interferences (e.g. Villena et al., 2012), when converting potentially PAN, HONO, HNO_3, etc. to NO, NO_2 concentrations were possibly overestimated. This overestimation of NO_2 would lead through its reaction with ozone to overestimate NO_3 concentration profiles. In order to largely account for uncertainties due to this potential overestimation of NO_2, NO_3 concentration profiles were modeled by multiplying and dividing NO_2 concentrations values by a factor of 2, leading proportionally to the same variation (i.e. a factor of 2) in the corresponding profiles. Note that the high concentration of NO_2 observed between July the 6th and 7th were related to a close harvesting episode in a field next to the site combined with easterly winds.

Calculated NO_3 concentrations within the canopy for the whole campaign are proposed in Fig. 1. Daily maxima ranged from nearly null to 0.10 ppt with an average daily maxima of 0.03 ppt, which is consistent with the observation that these concentrations were below the limit of detection of the IBBCEAS instrument along the campaign.

Surprisingly, daily maxima of NO_3 were observed during daytime. Considering this unusual observation, it was decided to validate - a posteriori - the NO_3 concentration calculation methodology used in the present study, by applying it to other datasets from previous campaigns carried out in a similar environment. Our choice focused on a boreal forested site, at the SMEAR II station, Hyytiälä, southern Finland, with one dataset from the HUMMPA-COPEC-10 campaign, performed in summer 2010 (Yassaa et al., 2012; Hens et al., 2014; Mogensen et al., 2015) and one gathering some ambient measurements monitored in summer 2019 (Li et al., 2020a)). In both cases, NO_3 concentrations were found to be maximum at nighttime, as usually observed.

Many reasons may explain the unexpected daytime maximum NO_3 concentrations observed during the LANDEX episode 1 campaign. Firstly, ozone concentrations often decreased to nearly zero at night during the campaign. Secondly, monoterpenes presented their highest concentrations during the night, justifying the low NO_3 profile due to their high reactivity with nitrate radicals. This observation could also be explained by the significant increase of relative humidity at night which is favourable to N_2O_5 hydrolysis and by the lower photolysis of NO_3 and the weak formation of NO (lowering the (NO_3 + NO) reaction loss) during the day in the forest cover. This is to be brought closely to model studies which suggested that during the day, in low luminosity conditions under the canopy, NO_3 oxidation may be an important sink for monoterpenes (which implies non-negligible production of NO_3 radicals) (Forkel et al., 2006; Fuentes et al., 2007). Finally, during the day, Liebmann et al. (2019) also recently observed more than 20% of

production of alkylnitrates from NO_3-initiated oxidation of BVOCs, corroborating the potential importance of daytime NO_3 concentrations under the canopy. In addition, note that Li et al. (2020b) also observed the formation of some monoterpene-derived organic nitrates ($C_{10}H_{15}NO_7$ for instance) during the CERVOLAND campaign at Bilos during daytime but did not succeed to evaluate the main processes governing such a formation. All these detailed and independent arguments strongly support the estimation of this unusual NO_3 concentration profile proposed in this study.

The evolution of monoterpene concentrations was comparable to previous measurements conducted at the same site during the LANDEX Episode 0 campaign in summer 2015 (Kammer et al., 2018). Sesquiterpenes (SQTs) were measured at this site for the first time during this study. Their concentrations followed the same diurnal pattern than MTs, β-caryophyllene representing around 40% of the total SQT concentration measured at *m/z* 205 by PTR-MS. Sesquiterpene concentrations were in the range (121 ± 85) ppt on average during the campaign. These values are much higher than at similar sites as in boreal forest (28 ppt) (Hellén et al., 2018) or for the conifer Blodgett Forest (44 ppt) in California (Bouvier-Brown et al., 2009).

Diurnal variations of isoprene and linalool exhibited maxima (1.1 ppb and 0.2 ppb on average, respectively) between 12:00 and 16:00 UTC. This behaviour is explained by light-and temperature-dependent emissions from plants as reported in the literature (Laothawornkitkul et al., 2009; Niinemets et al., 2010). Isoprene concentrations were surprisingly high for a maritime pine forest. Possible sources were associated to the large presence of gorse (*Ulex europaeus* L.), known to be an efficient isoprene emitter (Boissard et al., 2001), but also may have been emitted by other undergrowth plants (grass (*Molinia caerulea* (L.) Moench) and heather (*Calluna vulgaris* (L.) Hull)). Linalool was also measured at this site for the first time. Its presence could be due to biotic stress on some of the maritime pines (Nagnan and Clement, 1990; Kleinhentz et al., 1999). Isoprene concentrations were comparable to those observed for instance in ponderosa forest (1.9 ppbv in average in the afternoon) (Beaver et al., 2012). Tropical forests as in Amazonia present higher isoprene concentration levels at 24 m height with values (in average) of (19.9 ± 0.2) ppb but similar values as here at 12 m (1.1 ± 0.5 ppb). At Borneo, high concentrations of isoprene were observed with values up to 7 ppbv during the day (Edwards et al., 2013). In a boreal forest, isoprene concentrations were reported to be lower than in Bilos (i.e. around 100 ppt during the summer 2012 and less during the 2014 and 2015 years) (Hellén et al., 2018).

Pinonaldehyde and nopinone ((77 ± 74) ppt and (108 ± 149) ppt on average, respectively) are well-known oxidation products of α- and β-pinene, respectively. These compounds presented similar concentration profiles, with maxima of concentrations delayed by approximately 90 min from those of their pinene precursors, whatever the observation height. Their concentrations were larger during the "strong oxidation" periods, demonstrating the importance of reactive processes in this forest. Methylvinylketone and methacrolein (MVK + MACR) concentrations ((220 ± 375) ppt on average) also presented similar evolution as their precursor (i.e. isoprene) but in contrast to oxidation products from monoterpenes, no time delay was observed, likely due to the fast reactivity of isoprene with OH. This is supported by a higher ratio (MVK + MKA)/isoprene during the high oxidation periods.

3.2. On-site reactivity of BVOCs with the main atmospheric oxidants

As described in Sections 2.3 and 2.4, the role of BVOCs on the photochemistry occurring in the atmosphere of this forest was investigated by calculating the total reactivity considering their measured concentrations and the reaction rate constants with each of the three oxidants OH, O_3 and NO_3 (Eq. (1)). As seen in Fig. 3a and b, the average diurnal variability of BVOCs and total OH reactivity present similar distributions.

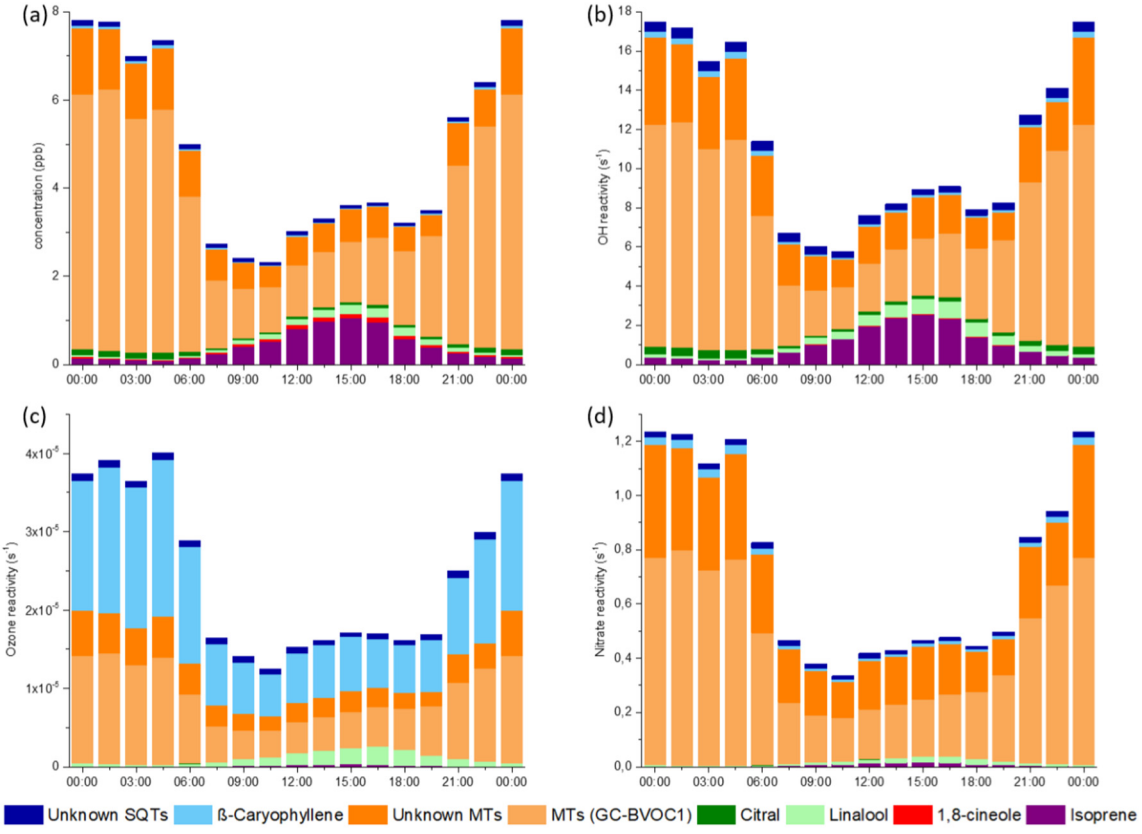

Fig. 3. Average diurnal variations of (a) measured BVOC concentrations, (b) total OH reactivity, (c) total O_3 reactivity and (d) total NO_3 reactivity with BVOCs at 6 m a.g.l. (under the canopy) during the LANDEX Episode 1 field campaign in 2017. SQTs: sesquiterpenes; MTs: monoterpenes. The data shown is based on a campaign average.

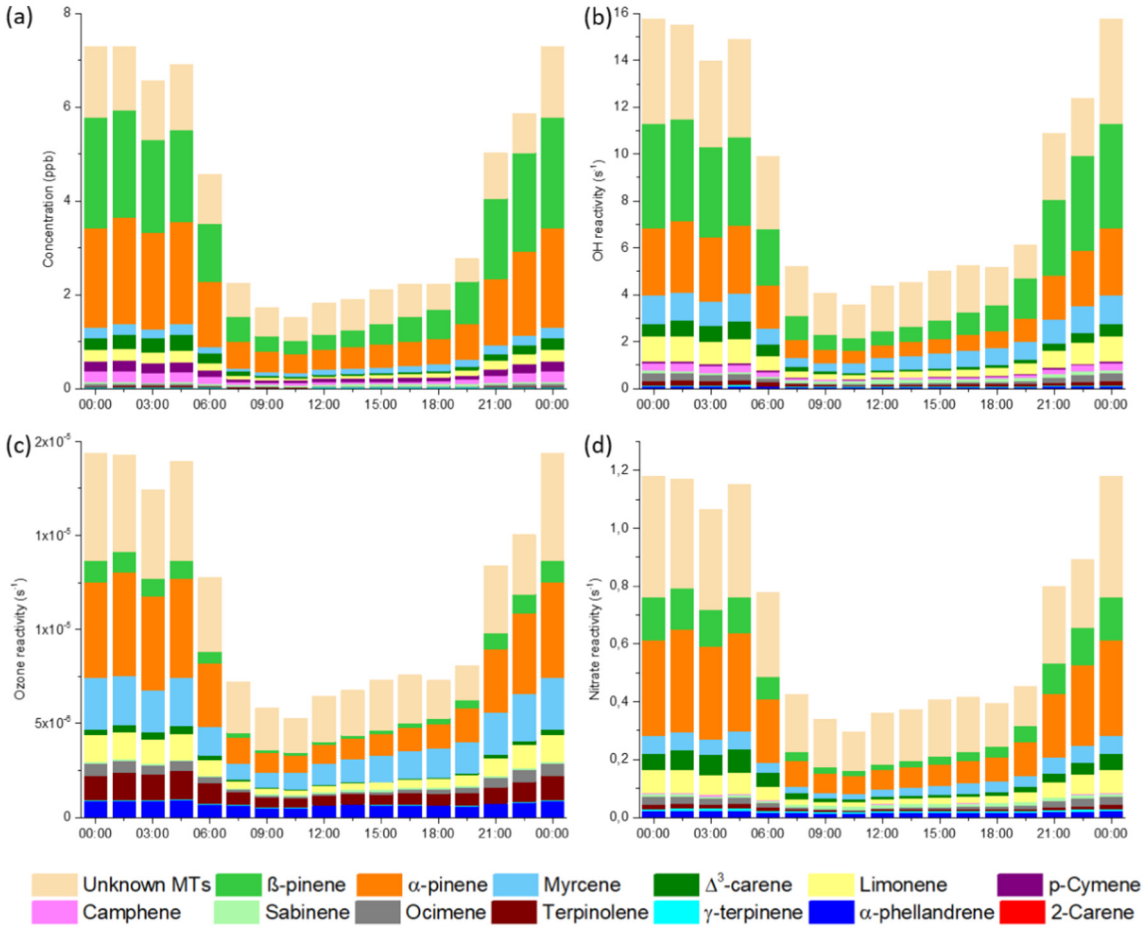

Fig. 4. Average diurnal variations of (a) measured MT concentrations, (b) total OH reactivity, (c) total O_3 reactivity and (d) total NO_3 reactivity, with monoterpenes at 6 m a.g.l (under the canopy) during the LANDEX Episode 1 field campaign in 2017. MTs: monoterpenes. The data shown is based on a campaign average.

Indeed, the highest reactivity of OH occurs during nighttime when the highest concentrations of BVOCs are observed (small range of BVOC reaction rate constants with OH). Such evolutions are consistent with previous observations reported by Carslaw et al. (2001), Hakola et al. (2012), Hellén et al. (2018) and Yáñez-Serrano et al. (2018) in forested environments.

At Bilos, monoterpenes accounted for up to 90% of the OH reactivity due to BVOCs at night and at least 60% during daytime. Isoprene and linalool also contributed significantly during daytime, with respective contributions of 20% and 10%. β-caryophyllene and other "unknown" sesquiterpenes contributed 2 times more to the total OH reactivity than to the total BVOC concentration. But their contribution to OH reactivity was still at least 12 times smaller than that of monoterpenes. Hakola et al. (2012) and more recently Hellén et al. (2018) have also observed that sesquiterpenes were impacting relatively largely the reactivity despite their low concentration in boreal forests.

α- and β-pinene, limonene and Δ^3-carene were found to contribute more to the total monoterpene concentration as well as the total OH reactivity during the night than during daytime, inversely to unknown MTs, myrcene, sabinene, camphene, γ-terpinene and α-phellandrene (Fig. 4a and b). For the other monoterpenes, no significant diurnal variation of their contributions was observed. "Unknown" MTs accounted for 15–35% of the calculated total OH reactivity for MTs (Fig. 4). Their contribution could reach up to 61% by considering they are highly reactive monoterpenes such as α-terpinene or α-phellandrene. Contributions of α- and β-pinene to the total monoterpene concentration were respectively higher by a factor of 2 and 1.5 than to the total OH reactivity induced by monoterpenes only (Figs. 3 and 4). This may be explained by their relatively low rate constants with OH compare to other MTs. In contrast, the contributions of myrcene, camphene, limonene, α-phellandrene, terpinolene and γ-terpinene were 2–3 times higher than expected regarding their concentrations due to their higher rate constant with OH.

As previously observed for OH, the ozone reactivity due to BVOCs was larger (here around 2 times) during nighttime (see Fig. 3). Note that the reaction of O_3 with NO accounted for 60–90% of the total ozone loss rate due to a high rate constant for this reaction ($k = 1.9 \times 10^{-14}$ cm^3 molecule^{-1} s^{-1} at 298 K). Sesquiterpenes and monoterpenes contributed equally to the BVOC ozone reactivity, even if the concentrations of MTs were up to 30 times larger than those of SQTs (Fig. 3c and a). This is due to the large reactivity of ozone with β-caryophyllene, representing 90% of total sesquiterpene reactivity. If we considered that unknown sesquiterpenes are composed of highly reactive sesquiterpenes such as α-humulene or β-caryophyllene, unknown SQT will contribute to 50% of the total sesquiterpene reactivity and highlight the role of SQTs on local ozone depletion. Linalool, which is emitted during daytime, accounted for 10% of the total ozone reactivity from BVOCs (Fig. 3).

The analysis of different MT contribution to the reactivity (Fig. 4) shows that six monoterpenes contributed for 60%–75% to the ozone reactivity: α-pinene, β-pinene, myrcene, limonene, terpinolene and α-phellandrene. α-pinene, β-pinene, myrcene and limonene were four of the six most abundant monoterpenes measured in this forest. For significantly less abundant MTs like terpinolene and α-phellandrene, high rate constant with ozone (respectively $k = 1.6 \times 10^{-15}$ cm^3 molecule^{-1} s^{-1} and $k = 2.9 \times 10^{-15}$ cm^3 molecule^{-1} s^{-1} at 298 K) leads to high relative reactivity. The α- and β-pinene contributions to the MT ozone reactivity were respectively a factor of 2 and 5 lower

than their contribution to the total MT concentration. In contrast, myrcene, terpinolene and α-phellandrene contributed respectively 3, 12 and 17 times more to the MT ozone reactivity than to the total MT concentration. The "unknown" fraction of MTs contributed to 20–30% of this total ozone reactivity (Fig. 4c), with a higher contribution during daytime. However, this estimation depends on the assigned rate constant value. For instance, if "unknown" MT would have been considered as reactive as α-terpinene they would have contributed up to 88% of monoterpenes reactivity.

Similar observations were recently reported by Hellén et al. (2018) and Yáñez-Serrano et al. (2018) for highly reactive monoterpenes such as α-terpinene. This compound was measured during the LANDEX Episode 1 field campaign but with a signal to noise ratio too low to be considered in this analysis. If considered, α-terpinene would contribute to 40% of the total MT ozone reactivity and to 6% of the total ozone reactivity (including all BVOCs and NO), which is equivalent to the contribution of β-caryophyllene.

The total nitrate reactivity with BVOCs was mainly due to monoterpenes (80–95%) (Fig. 3d). "Unknown" MTs were among the main contributors to nitrate reactivity (25–40%). This contribution could reach 90% if we considered they were highly reactive monoterpenes such as α-terpinene. As for OH, the five most abundant MTs (Fig. 4d) were α-pinene, β-pinene, myrcene, limonene, Δ^3-carene. Interestingly, α-phellandrene which was one of the less abundant monoterpenes in ambient air (< 1%) contributed to 3–8% of the total nitrate reactivity due to monoterpenes.

The calculations discussed above stress the need to also focus on less abundant compounds as they can have a significant impact on the oxidative capacity of the atmosphere. Indeed pinenes and limonene only are not sufficient to stand for monoterpene reactivity when other compounds such as α-phellandrene, myrcene or terpinolene are present.

3.3. BVOC consumption by atmospheric oxidants

The contribution of each oxidant (OH, O_3 and NO_3) to the total consumption rate of specific BVOCs was calculated using Eq. (4). As described in Section 2.4, two scenarios of OH estimations (upper and lower limits) were evaluated. On Fig. 5 are reported diurnal variations of the contributions of the three atmospheric oxidants to the total consumption rate of α-pinene, β-pinene, β-caryophyllene, Δ^3-carene and citral chosen as representative of the 5 reactivity groups of species (see below) within the forest cover for the upper limit of OH. More illustrations for each class of compounds and for both upper and lower OH limits are provided in the supplement, Figs. S4-1, S4-2 and S4-3.

BVOCs can be divided into 5 groups based on the observed removal patterns (contributions of oxidants) along the campaign. The first group is composed of α-pinene, myrcene, linalool, limonene, terpinolene and ocimene (Figs. S4-1 and 5). All these compounds mainly reacted with ozone during both daytime and nighttime periods. The OH oxidation pathway contributed to 45% and 20% of the total BVOC consumption rate for the highest and lowest OH scenarios (including the related effects of the NO_3 concentration uncertainties) respectively during daytime. Their oxidation by nitrate radicals represented less than 10% of each compound consumption (considering a reasonable factor ± 2 uncertainty on NO_3 calculated concentration values).

The second group is composed of β-pinene and isoprene. These two compounds mainly reacted with OH during daytime (up to 85% under high OH and 80% under low OH) but also exhibited a significant loss due to their reaction with ozone (up to 15% under high OH and 35%

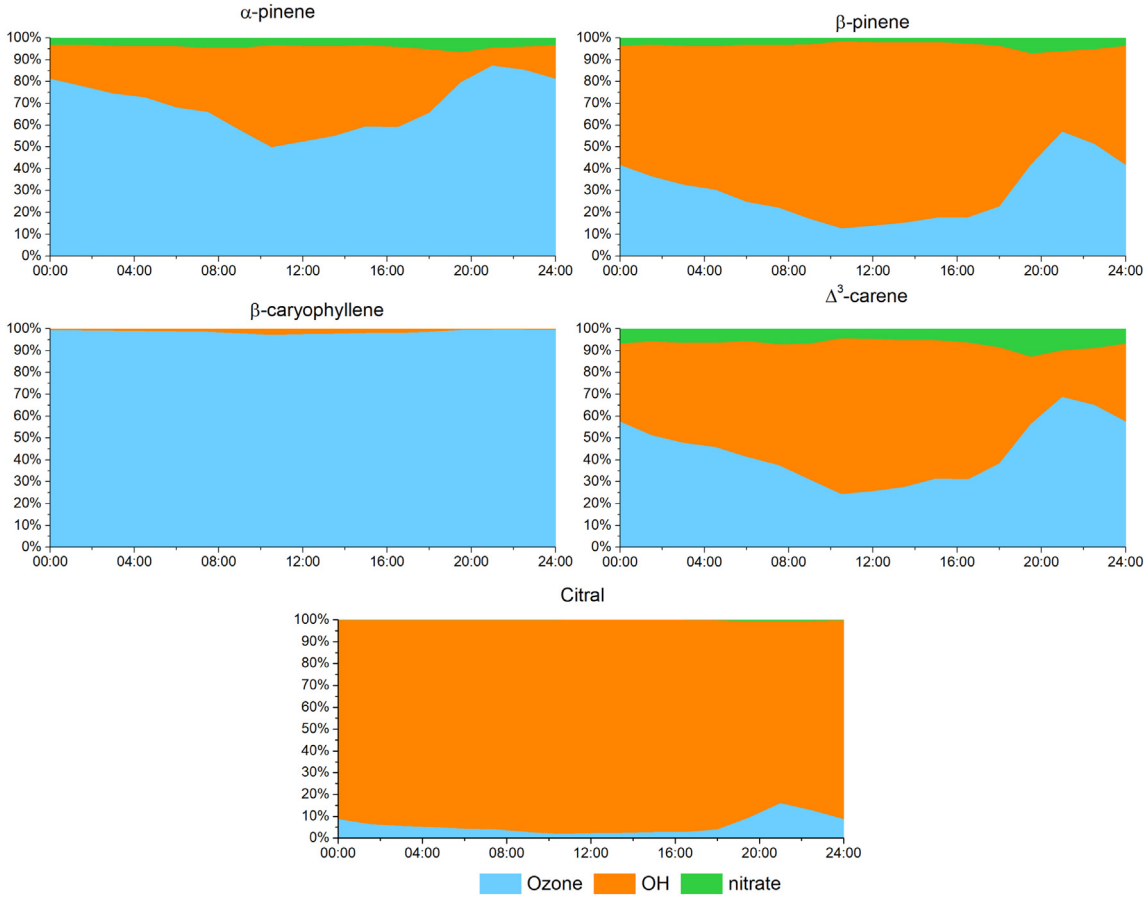

Fig. 5. Averaged diurnal variations of the contribution of each atmospheric oxidant to α-pinene, β-pinene, β-caryophyllene, Δ^3-carene and citral consumption rates at 6 m a.g.l. (under the canopy), considering an upper limit for OH concentrations (see text).

under low OH). During the night, the ozone contribution could reach up to 35% for isoprene (Fig. S4-2) and up to 45% for β-pinene (Fig. 5), considering both OH concentrations scenarios. Similarly to the first group, the contribution of the NO_3 pathway to the total loss of these compounds was lower than 10% in both OH conditions.

The third group is composed of β-caryophyllene and α-phellandrene. These compounds almost exclusively reacted with ozone during both daytime and nighttime for both OH scenarios and the contributions of their reactions with OH and NO_3 were always lower than 10% and 5% respectively for both OH scenarios (Figs. 5 and S4-3).

The fourth group is composed of Δ^3-carene, γ-terpinene and sabinene. They mainly reacted diurnally with OH in both scenarios (Figs. 5 and S4-2). During the night, their reactions with ozone could equal or even overpass reaction with OH. Oxidation by nitrate represented 7–25% of the quoted monoterpene consumption.

The fifth and last group was composed of 1,8-cineole, citral, camphene and p-cymene. These compounds mainly reacted with OH whatever the conditions, the contributions of ozone and nitrate radical reactions being always lower than 10% (Figs. 5 and S4-3).

To get a better assessment of the influence of the nitrate radical, BVOC total consumption was calculated including high OH / low NO_3 and low OH / high NO_3 concentration scenarios. This change is presented for five compounds considered to be the most influenced by a variation of NO_3 concentration (Fig. S4–4). Note that compounds of the fourth group were the most sensitive to the nitrate concentration and that the nitrate reactivity could sometimes be the second most important oxidative process leading to their consumption.

Similarly to the conclusion of the previous section, it can be highlighted that modelling the MT reactivity in the atmosphere using only β-pinene (group 2), α-pinene and limonene (group 1) as surrogates might not be enough in the presence of compounds from other groups such as Δ^3-carene, camphene and α-phellandrene presenting different reactivity patterns with oxidants. Interestingly, this classification could be used to choose one reference compound per group to model the BVOC reactivity.

3.4. BVOC loss rate within and above the canopy

In order to evaluate the amount of BVOCs oxidized in the forest, individual loss rates (LR_{VOC}) were calculated for isoprene, MTs, SQTs, citral, linalool and eucalyptol, as described in Section 2.5.

As seen in Figs. 6 and S5, daily average of LR_{VOC} were around 1.5 faster for monoterpenes than for sesquiterpenes, for both low OH and high OH conditions. The SQT and MT total loss rates were higher during daytime, especially between 12:00 and 16:30 UTC, for both strong and low oxidation periods (Figs. 6 and S6). It is worth noting that the loss rates reported in Fig. 6 correspond to the product of both the oxidant reactivity (expressed in s^{-1}) and the oxidant concentration (expressed in molecule cm^{-3}).

Isoprene and linalool loss rates were lower than for MTs and SQTs but were still significant during daytime (12 and 18% of the MT loss rate on a 24-h average, respectively). This is related with isoprene and linalool light- and temperature-dependent emissions. For monoterpenes, loss rate due to OH and ozone were fairly similar during daytime while ozone related loss rate is dominant during the night-time. The contribution of the reaction with NO_3 remained low (approximatively 5% of the total LR). For sesquiterpenes, the contribution of ozone reactions was major compared to those with OH and NO_3.

The total amount of BVOC oxidized by the three major oxidants has been calculated for a period of 14 days (30th June to 13th July 2017) as described in Section 2.5. Results are reported in Fig. 7 with separation of nighttime and daytime contributions.

Following the approach developed in the recent paper by Edwards et al. (2017) on the transitions from high- to low-NOx control of

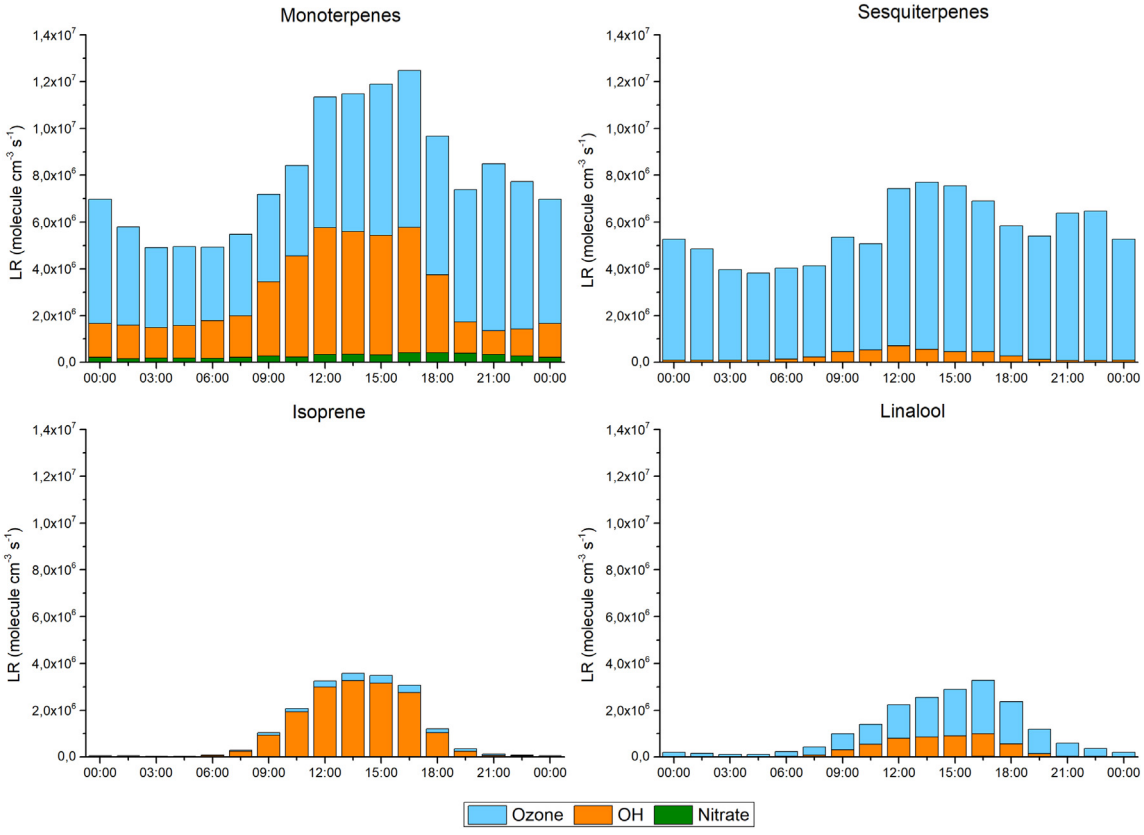

Fig. 6. Diurnal variations of BVOC loss rates (LRVOC) from monoterpenes, sesquiterpenes, isoprene and linalool for high OH conditions at 6 m a.g.l. (under the canopy) averaged over the LANDEX episode 1 campaign in 2017.

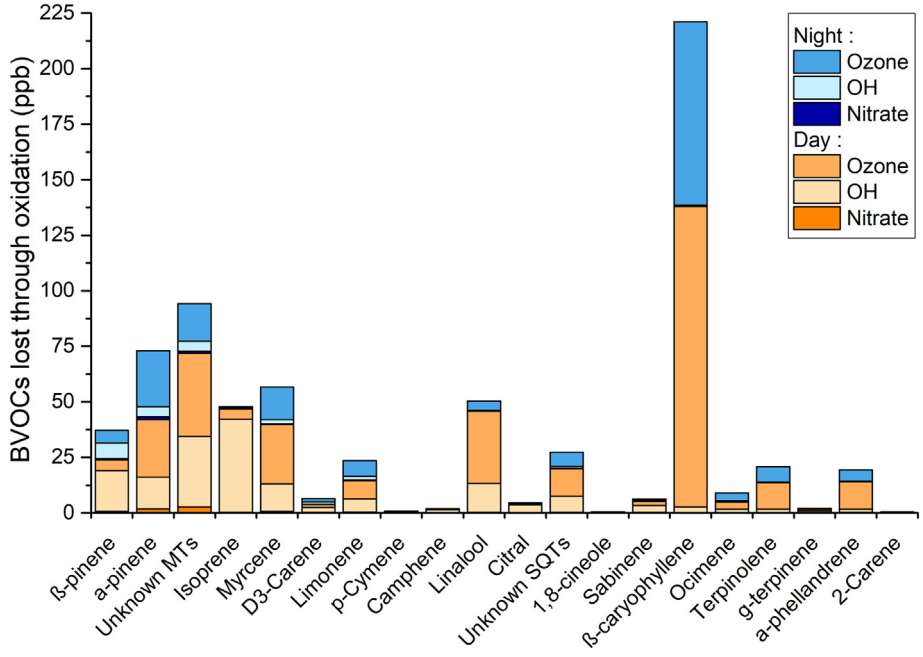

Fig. 7. Calculated concentrations (in ppb) of BVOC oxidized during the 30th June to 13th July 2017 period with the contribution of the three main atmospheric oxidants, during nighttime and daytime, for the high OH concentration scenario at 6 m a.g.l. (under the canopy). VOCs are classified from the most to the less abundant in ambient air (from left to right).

nighttime oxidation, proposing that nighttime NO_x to BVOC ratios may help to characterize the dominant chemical processes in different environments, the mean value of [NOx]/[BVOCs] was determined during the campaign to be equal to (0.27 ± 0.16) during nighttime, i.e. below 0.5, reinforcing the fact that nighttime oxidation of BVOCs during LANDEX Ep. 1 was NO_x-limited and therefore ozone-dominant, as previously demonstrated.

The reaction generating the largest consumption of BVOCs was that of β-caryophyllene with O_3, as also recently observed in a boreal forest by Hellén et al. (2018). Note that if β-caryophyllene was observed as the most emitted sesquiterpene, its emissions were always very weak compared to other BVOCs but, on the other hand, it reacts very fast with ozone (around 100 times faster than α-pinene), leading to the fact that its single ozonolysis was the most efficient process among all other BVOC reactions. The sum of individual contribution of α-pinene, β-pinene and limonene to the total loss of BVOCs, which are often used to represent monoterpenes in reactivity models, appeared here relatively low (around 30%). Myrcene, terpinolene and α-phellandrene reactions with ozone contributed around 22% to the total loss of monoterpenes. This is an important point to be considered regarding their SOA formation rate potentially higher than α-pinene, β-pinene and limonene, which are yet so far the most studied compounds in chamber experiments (Hallquist et al., 2009). Finally, the reaction of isoprene with OH was the third biggest contributor to BVOC oxidation despite the quasi monospecific composition of this forest, i.e. pine trees, characterized as strong emitters of pinenes. All the BVOC reactions with nitrate did not have a significant influence on the BVOC consumption: an increase of 2 times of its concentration leads to just an increase of 4% of the BVOC consumed, to be compared when using both scenarios of OH leading to an increase of 11%. Compounds the most influenced by the nitrate reactivity (i.e. belonging to the fourth group presented in Section 3.3) are logically the less reactive with ozone and OH, their influence being tiny on the total BVOC lost. However, if varying the nitrate concentration had a small influence on BVOC consumption in this work, it may still impact the formation of nitrate secondary products as recently demonstrated by Liebmann et al. (2019).

Relative global BVOC reactivities (including isoprene, MTs, SQTs and OBVOCs) were estimated on a daily average basis from the Fig. 6. Values obtained in this work (with O_3: 3.6×10^{-4} s^{-1}, OH: 13.3 s^{-1} and NO_3: 3.5 s^{-1}) for a pine tree forest were compared to modeled and measured reactivities reported in two previous studies at SMEAR II in southern Finland. During the HUMPPA-COPEC-10 campaign in summer 2010, Mogensen et al. (2015) reported relative reactivities values of 2×10^{-5} s^{-1}, 3 s^{-1} and 0.07 s^{-1} with O_3, OH and NO_3 respectively, i.e. a factor of 18, 4.5 and 50 lower than those estimated in this work. More, in the second study, presenting similar ozone mean concentrations, nitrate concentrations less than 0.2 ppt and maximal OH around 8×10^5 molecule cm^{-3} (Hellén et al., 2018), the mean reactivity of BVOCs was also much slower, i.e. about 45 times with O_3, around a factor 8 with OH and 22 times with NO_3 than during the LANDEX Ep. 1 campaign. The main points supporting such high reactivity observed at Bilos were the larger BVOC concentration values, due to the forest specificity (mainly its density and monospecificity) and the meteorological conditions, but also to the larger speciation of BVOCs measured in this work (more than 20), including some monoterpenes (like α-phellandrene, γ-terpinene and terpinolene) presenting much faster reaction kinetics with atmospheric oxidants than the average MTs, even if present at low concentrations.

In order to illustrate the influence of the vertical BVOC concentration gradient (i.e. in the forest cover or above the canopy) on the BVOC loss rates, 7 BVOCs (isoprene, α-pinene, β-pinene, myrcene, Δ^3-carene, limonene + cis-ocimene), measured at 6 m and 12 m a.g.l., were considered in Fig. 8.

Considering the different BVOC oxidation rates, the amount of BVOC oxidized was similar or larger in the forest cover than above the canopy, with the exception of isoprene (Fig. 8). While isoprene concentrations were similar at both heights, OH concentrations at 12 m were evaluated to be around 2 times higher than at 6 m where solar radiation is attenuated, explaining the difference for isoprene loss rate.

During daytime, monoterpene concentrations were around 30% lower (see Figs. 2 and S2) above than below the canopy, likely due to a larger dilution effect, to a smaller emission above and to the fact that monoterpenes from below the canopy might not be a potential input (as they already started to react). This increase in the monoterpene concentrations inside the cover led to higher MT loss rates. Such differences were higher during the night, more especially in stable (i.e. for mean $1/u^* \geq 5$ s m^{-1}) and warm (for mean $T \geq 19$ °C) atmospheric conditions (Bsaibes et al., 2020). Hence, monoterpene oxidation products were

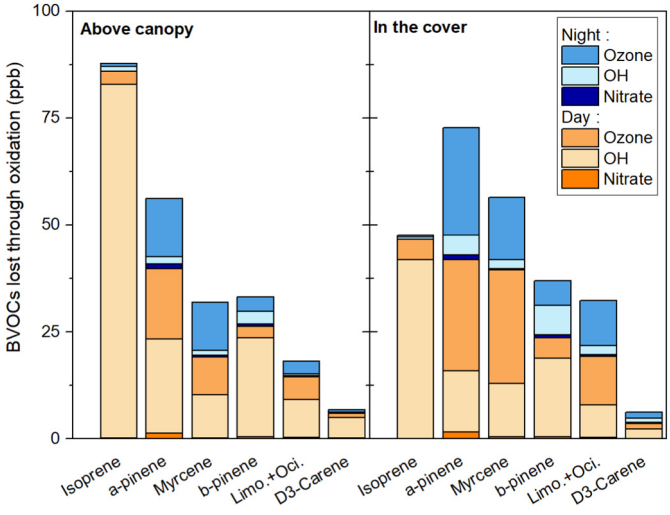

Fig. 8. Calculated concentrations (in ppb) of BVOC oxidized during all the campaign with the contribution of the three main atmospheric oxidants, during nighttime and daytime, above the canopy and under the forest cover, for the high OH concentration scenario. VOCs are classified from the most to the less abundant in ambient air (from left to right).

mainly formed within the cover, strengthening the observations reported by Kammer et al. (2018), showing that SOA formation processes mainly occurred below the canopy of the Landes forest. To corroborate the further influence of the monoterpene and other BVOC reactive pathways on SOA formation, a recent study by Li et al. (2020b) performed at the same site but in summer 2018 measured an extensive list of gaseous oxidation products, attempting the importance of oxidation processes at Bilos.

4. Conclusion

In this work, a large dataset of VOCs (including pinenes, carenes, terpinene, linalool, camphene, etc.) was measured at Bilos in the Landes forest to better assess the onsite reactivity of BVOCs with the three main oxidants (OH, O_3 and NO_3), in the cover and above the canopy. The approach was based on intensive concentration measurements and on calculations of depletion rates for both BVOCs and oxidants. Note that NO_3 was estimated to be unusually maximal during daytime.

Monoterpenes exhibited the highest concentrations, α-pinene and β-pinene representing 48% of the total of MTs. If isoprene was the third most abundant compound measured in the forest, highly reactive species were also monitored, such as β-caryophyllene.

The impact of the different BVOCs on the local atmospheric chemistry was evaluated. Monoterpenes dominated the OH and the NO_3 radical chemistry. During daytime, isoprene and linalool were also impacting the OH total reactivity with BVOCs. Due to their high reactivity with ozone, sesquiterpenes may play a role in the local ozone budget, despite their relatively low concentrations (32 times lower than MTs).

Monoterpene oxidation was dominated by OH during the day and by O_3 during the night. α-pinene and β-pinene contributed less than expected to the total oxidation flux of monoterpenes despite their high ambient concentrations. Less abundant but highly ozone-reactive compounds such as myrcene or terpinolene, can also significantly impact monoterpene oxidation processes and the formation of secondary products. A comparison of the BVOC reactivity observed above and below the forest canopy showed that the oxidation fluxes of monoterpenes and sesquiterpenes were larger below the canopy and likely led to a higher formation rate of secondary products in the cover, unlike isoprene.

If monoterpene reactive processes were responsible for most of oxidation products in the cover, the single reaction between β-caryophyllene and ozone was the most efficient among all. This approach also stresses out (i) the necessity to measure less abundant sesquiterpenes and reactive monoterpenes such as terpinolene and α-phellandrene, (ii) that only considering α-pinene, β-pinene and limonene as surrogate species for all monoterpenes in modelling studies might not be enough representative of the reality.

Finally, this study will help to select potential specific tracers (like 3-methyl-1,2,3-butane tricarboxylic acid (MTBCA), pinic and pinonic acids, etc.) of SOA formation in the Landes forest since the involvement of monoterpenes like β-pinene, α-pinene, myrcene, β-caryophyllene or linalool in reactive processes was clearly demonstrated and evaluated. The next step will consist in linking the atmospheric gas phase composition, the reactive processes highlighted in this work, with the particle composition to better understand the formation and fate of biogenic SOA in a temperate pine tree forest.

CRediT authorship contribution statement

KM, TL, SS and NL carried out GC-BVOC1, GC-NMHC measurements and provided analysed data. SB, FT and VG provided GC-BVOC2 analysed data. SD carried out PTR-MS and ozone measurements and provided the corresponding data. VM, MC, AG and JFD set up and carried out NO_3 concentration measurements with the IBBCEAS technique and mixing layer height measurements with the ceilometer. MAA, CS, SB and CH set up and carried out OH concentration measurements with the UL-FAGE instrument. JK and PMF provided NO_x data and meteorological parameters. EV, EP and PMF coordinated the LANDEX project and the logistics of all the field campaign. KM prepared the paper with all co-author contributions, mainly from EP, SD, SS, NL and EV.

Declaration of competing interest

The authors declare that they have no known competing financial interests or personal relationships that could have appeared to influence the work reported in this paper.

Acknowledgements

This study was supported by the French Environment and Energy Management Agency (ADEME), the CNRS INSU LEFE-CHAT program, and also benefitted from grants from the French National Research Agency (ANR) as part of the Investments for the Future Program (Cluster of Excellence COTE, ANR-10-LABX-45). The authors want to acknowledge the Bilos ICOS team (Christophe Chipeaux and Denis Loustau) for meteorological data and site availability.

Appendix A. Supplementary data

Supplementary data to this article can be found online at https://doi.org/10.1016/j.scitotenv.2020.144129.

References

Amedro, D., Miyazaki, K., Parker, A., Schoemaecker, C., Fittschen, C., 2012. Atmospheric and kinetic studies of OH and HO_2 by the FAGE technique. J. Environ. Sci. 24, 78–86. https://doi.org/10.1016/S1001-0742(11)60723-7.

Atkinson, R., Arey, J., 2003. Gas-phase tropospheric chemistry of biogenic volatile organic compounds: a review. Atmos. Environ. 37 (Supplement 2), 197–219. https://doi.org/10.1016/S1352-2310(03)00391-1.

Badol, C., Borbon, A., Locoge, N., Léonardis, T., Galloo, J.-C., 2004. An automated monitoring system for VOC ozone precursors in ambient air: development, implementation and data analysis. Anal. Bioanal. Chem. 378, 1815–1827. https://doi.org/10.1007/s00216-003-2474-0.

Beaver, M.R., Clair, J.M.St., Paulot, F., Spencer, K.M., Crounse, J.D., LaFranchi, B.W., Min, K.E., Pusede, S.E., Wooldridge, P.J., Schade, G.W., Park, C., Cohen, R.C., Wennberg, P.O., 2012. Importance of biogenic precursors to the budget of organic nitrates: observations of multifunctional organic nitrates by CIMS and TD-LIF during BEARPEX 2009. Atmos. Chem. Phys. 12, 5773–5785. https://doi.org/10.5194/acp-12-5773-2012.

Berresheim, H., Elste, T., Plass-Dülmer, C., Eiseleb, F.L., Tannerb, D.J., 2000. Chemical ionization mass spectrometer for long-term measurements of atmospheric OH and H_2SO_4. Int. J. Mass Spectrom. 202, 91–109. https://doi.org/10.1016/S1387-3806(00)00233-5.

Birmili, W., Berresheim, H., Plass-Dülmer, C., Elste, T., Gilge, S., Wiedensohler, A., Uhrner, U., 2003. The Hohenpeissenberg aerosol formation experiment (HAFEX): a long-term study including size-resolved aerosol, H_2SO_4, OH, and monoterpenes measurements. Atmos. Chem. Phys. 3, 361–376. https://doi.org/10.5194/acp-3-361-2003.

Boissard, C., Cao, X.-L., Juan, C.-Y., Hewitt, C.N., Gallagher, M., 2001. Seasonal variations in VOC emission rates from gorse (Ulex europaeus). Atmos. Environ. 35, 917–927. https://doi.org/10.1016/S1352-2310(00)00362-9.

Bouvier-Brown, N.C., Goldstein, A.H., Gilman, J.B., Kuster, W.C., de Gouw, J.A., 2009. In-situ ambient quantification of monoterpenes, sesquiterpenes, and related oxygenated compounds during BEARPEX 2007: implications for gas- and particle-phase chemistry. Atmos. Chem. Phys. 9, 5505–5518. https://doi.org/10.5194/acp-9-5505-2009.

Bsaibes, S., Al Ajami, M., Mermet, K., Truong, F., Batut, S., Hecquet, C., Dusanter, S., Léornadis, T., Sauvage, S., Kammer, J., Flaud, P.-M., Perraudin, E., Villenave, E., Locoge, N., Gros, V., Schoemaecker, C., 2020. Variability of OH reactivity in the Landes maritime Pine forest: results from the LANDEX campaign 2017. Atmos. Chem. Phys. 20, 1277–1300. https://doi.org/10.5194/acp-20-1277-2020.

Capes, G., Murphy, J.G., Reeves, C.E., McQuaid, J.B., Hamilton, J.F., Hopkins, J.R., Crosier, J., Williams, P.I., Coe, H., 2009. Secondary organic aerosol from biogenic VOCs over West Africa during AMMA. Atmos. Chem. Phys. 9, 3841–3850. https://doi.org/10.5194/acp-9-3841-2009.

Carslaw, N., Creasey, D.J., Harrison, D., Heard, D.E., Hunter, M.C., Jacobs, P.J., Jenkin, M.E., Lee, J.D., Lewis, A.C., Pilling, M.J., Saunders, S.M., Seakins, P.W., 2001. OH and HO2 radical chemistry in a forested region of north-western Greece. Atmos. Environ. 35, 4725–4737. https://doi.org/10.1016/S1352-2310(01)00089-9.

Di Carlo, P., Brune, W.H., Martinez, M., Harder, H., Lesher, R., Ren, X., Thornberry, T., Carroll, M.A., Young, V., Shepson, P.B., Riemer, D., Apel, E., Campbell, C., 2004. Missing OH reactivity in a forest: evidence for unknown reactive biogenic VOCs. Science 304, 722–725. https://doi.org/10.1126/science.1094392.

Dusanter, S., Stevens, P.S., 2017. Recent advances in the chemistry of OH and HO_2 radicals in the atmosphere: field and laboratory measurements. Advances in Atmospheric Chemistry. World Scientific, pp. 493–579 https://doi.org/10.1142/9789813147355_0007.

Edwards, P.M., Evans, M.J., Furneaux, K.L., Hopkins, J., Ingham, T., Jones, C., Lee, J.D., Lewis, A.C., Moller, S.J., Stone, D., Whalley, L.K., Heard, D.E., 2013. OH reactivity in a South East Asian tropical rainforest during the Oxidant and Particle Photochemical Processes (OP3) project. Atmos. Chem. Phys. 13, 9497–9514. https://doi.org/10.5194/acp-13-9497-2013.

Edwards, P.M., Aikin, K.C., Dube, W.P., Fry, J.L., Gilman, J.B., de Gouw, J.A., Graus, M.G., Hanisco, T.F., Holloway, J., Hübler, G., Kaiser, J., Keutsch, F.N., Lerner, B.M., Neuman, J.A., Parrish, D.D., Peischl, J., Pollack, I.B., Ravishankara, A.R., Roberts, J.M., Ryerson, T.B., Trainer, M., Veres, P.R., Wolfe, G.M., Warneke, C., Brown, S.S., 2017. Transition from high- to low-NOx control of night-time oxidation in the southeastern US. Nat. Geosci. 10, 490–495. https://doi.org/10.1038/ngeo2976.

Forkel, R., Klemm, O., Graus, M., Rappenglück, B., Stockwell, W.R., Grabmer, W., Held, A., Hansel, A., Steinbrecher, R., 2006. Trace gas exchange and gas phase chemistry in a Norway spruce forest: a study with a coupled 1-dimensional canopy atmospheric chemistry emission model. Atmos. Environ. 40, S28–S42. https://doi.org/10.1016/j.atmosenv.2005.11.070.

Freney, E., Sellegri, K., Chrit, M., Adachi, K., Brito, J., Waked, A., Borbon, A., Colomb, A., Dupuy, R., Pichon, J.-M., Bouvier, L., Delon, C., Jambert, C., Durand, P., Bourianne, T., Gaimoz, C., Triquet, S., Féron, A., Beekmann, M., Dulac, F., Sartelet, K., 2018. Aerosol composition and the contribution of SOA formation over Mediterranean forests. Atmos. Chem. Phys. 18, 7041–7056. doi:105194/acp-18-7041-2018.

Fuentes, J.D., Wang, D., Bowling, D.R., et al., 2007. Biogenic hydrocarbon chemistry within and above a mixed deciduous forest. J. Atmos. Chem. 56, 165–185. https://doi.org/10.1007/s10874-006-9048-4.

Gauss, M., Myhre, G., Isaksen, I.S.A., Grewe, V., Pitari, G., Wild, O., Collins, W.J., Dentener, F.J., Ellingsen, K., Gohar, L.K., Hauglustaine, D.A., Iachetti, D., Lamarque, F., Mancini, E., Mickley, L.J., Prather, M.J., Pyle, J.A., Sanderson, M.G., Shine, K.P., Stevenson, D.S., Sudo, K., Szopa, S., Zeng, G., 2006. Radiative forcing since preindustrial times due to ozone change in the troposphere and the lower stratosphere. Atmos. Chem. Phys. 6, 575–599. https://doi.org/10.5194/acp-6-575-2006.

Gómez-González, Y., Wang, W., Vermeylen, R., Chi, X., Neirynck, J., Janssens, I.A., Maenhaut, W., Claeys, M., 2012. Chemical characterisation of atmospheric aerosols during a 2007 summer field campaign at Brasschaat, Belgium: sources and source processes of biogenic secondary organic aerosol. Atmos. Chem. Phys. 12, 125–138. https://doi.org/10.5194/acp-12-125-2012.

Griffith, S.M., Hansen, R.F., Dusanter, S., Stevens, P.S., Alaghmand, M., Bertman, S.B., Carroll, M.A., Erickson, M., Galloway, M., Grossberg, N., Hottle, J., Hou, J., Jobson, B.T., Kammrath, A., Keutsch, F.N., Lefer, B.L., Mielke, L.H., O'Brien, A., Shepson, P.B., Thurlow, M., Wallace, W., Zhang, N., Zhou, X.L., 2013. OH and HO_2 radical chemistry during PROPHET 2008 and CABINEX 2009 – part 1: measurements and model comparison. Atmos. Chem. Phys. 13, 5403–5423. https://doi.org/10.5194/acp-13-5403-2013.

Gros, V., Gaimoz, C., Herrmann, F., Custer, T., Williams, J., Bonsang, B., Sauvage, S., Locoge, N., Gros, V., Gaimoz, C., Herrmann, F., Custer, T., Williams, J., Bonsang, B., Sauvage, S., Locoge, N., 2011. Volatile organic compounds sources in Paris in spring 2007. Part I: qualitative analysis. Environ. Chem. 8, 74–90. https://doi.org/10.1071/en10068.

Hakola, H., Hellén, H., Hemmilä, M., Rinne, J., Kulmala, M., 2012. Atmospheric Chemistry and Physics. 12 (23), 11665–11678. https://doi.org/10.5194/acp-12-11665-2012.

Hallquist, M., Wenger, J.C., Baltensperger, U., Rudich, Y., Simpson, D., Claeys, M., Dommen, J., Donahue, N.M., George, C., Goldstein, A.H., Hamilton, J.F., Herrmann, H., Hoffmann, T., Iinuma, Y., Jang, M., Jenkin, M.E., Jimenez, J.L., Kiendler-Scharr, A., Maenhaut, W., McFiggans, G., Mentel, Th.F., Monod, A., Prévôt, A.S.H., Seinfeld, J.H., Surratt, J.D., Szmigielski, R., Wildt, J., 2009. The formation, properties and impact of secondary organic aerosol: current and emerging issues. Atmos. Chem. Phys. 9, 5155–5236. https://doi.org/10.5194/acp-9-5155-2009.

Hansen, R.F., Griffith, S.M., Dusanter, S., Rickly, P.S., Stevens, P.S., Bertman, S.B., Carroll, M.A., Erickson, M.H., Flynn, J.H., Grossberg, N., Jobson, B.T., Lefer, B.L., Wallace, H.W., 2014. Measurements of total hydroxyl radical reactivity during CABINEX 2009 – part 1: field measurements. Atmos. Chem. Phys. 14, 2923–2937. https://doi.org/10.5194/acp-14-2923-2014.

Hellén, H., Praplan, A.P., Tykkä, T., Ylivinkka, I., Vakkari, V., Bäck, J., Petäjä, T., Kulmala, M., Hakola, H., 2018. Long-term measurements of volatile organic compounds highlight the importance of sesquiterpenes for the atmospheric chemistry in boreal forest. Atmos. Chem. Phys. 2018, 13839–13863. https://doi.org/10.5194/acp-18-13839-2018.

Hens, K., Novelli, A., Martinez, M., Auld, J., Axinte, R., Bohn, B., Fischer, H., Keronen, P., Kubistin, D., Nölscher, A.C., Oswald, R., Paasonen, P., Petäjä, T., Regelin, E., Sander, R., Sinha, V., Sipilä, M., Taraborrelli, D., Tatum Ernest, C., Williams, J., Lelieveld, J., Harder, H., 2014. Observation and modelling of HO_x radicals in a boreal forest. Atmos. Chem. Phys. 14, 8723–8747. https://doi.org/10.5194/acp-14-8723-2014.

Hoffmann, T., Odum, J.R., Bowman, F., Collins, D., Klockow, D., Flagan, R.C., Seinfeld, J.H., 1997. Formation of organic aerosols from the oxidation of biogenic hydrocarbons. J. Atmos. Chem. 26, 189–222. https://doi.org/10.1023/A:1005734301837.

Houweling, S., Dentener, F., Lelieveld, J., 1998. The impact of nonmethane hydrocarbon compounds on tropospheric photochemistry. J. Geophys. Res. Atmospheres 103, 10673–10696. https://doi.org/10.1029/97JD03582.

Kaiser, J., Skog, K.M., Baumann, K., Bertman, S.B., Brown, S.B., Brune, W.H., Crounse, J.D., de Gouw, J.A., Edgerton, E.S., Feiner, P.A., Goldstein, A.H., Koss, A., Misztal, P.K., Nguyen, T.B., Olson, K.F., St. Clair, J.M., Teng, A.P., Toma, S., Wennberg, P.O., Wild, R.J., Zhang, L., Keutsch, F.N., 2016. Speciation of OH reactivity above the canopy of an isoprene-dominated forest. Atmos. Chem. Phys. 16, 9349–9359. https://doi.org/10.5194/acp-16-9349-2016.

Kammer, J., Perraudin, E., Flaud, P.-M., Lamaud, E., Bonnefond, J.M., Villenave, E., 2018. Observation of nighttime new particle formation over the French Landes forest. Sci. Total Environ. 621, 1084–1092. https://doi.org/10.1016/j.scitotenv.2017.10.118.

Kammer, J., Flaud, P.-M., Chazeaubeny, A., Ciuraru, R., Le Menach, K., Geneste, E., Budzinski, H., Bonnefond, J.-M., Lamaud, E., Perraudin, E., Villenave, E., 2020. Biogenic volatile organic compounds (BVOCs) reactivity related to new particle formation (NPF) over the Landes forest. Atmos. Res. 237, 104869. https://doi.org/10.1016/j.atmosres.2020.104869.

Kaser, L., Karl, T., Schnitzhofer, R., Graus, M., Herdlinger-Blatt, I.S., DiGangi, J.P., Sive, B., Turnipseed, A., Hornbrook, R.S., Zheng, W., Flocke, F.M., Guenther, A., Keutsch, F.N., Apel, E., Hansel, A., 2013. Comparison of different real time VOC measurement techniques in a ponderosa pine forest. Atmos. Chem. Phys. 13, 2893–2906. https://doi.org/10.5194/acp-13-2893-2013.

Kazil, J., Stier, P., Zhang, K., Quaas, J., Kinne, S., O'Donnell, D., Rast, S., Esch, M., Ferrachat, S., Lohmann, U., Feichter, J., 2010. Aerosol nucleation and its role for clouds and Earth's radiative forcing in the aerosol-climate model ECHAM5-HAM. Atmos. Chem. Phys. 10, 10733–10752. https://doi.org/10.5194/acp-10-10733-2010.

Kesselmeier, J., Staudt, M., 1999. Biogenic volatile organic compounds (VOC): an overview on emission, physiology and ecology. J. Atmos. Chem. 33, 23–88. https://doi.org/10.1023/A:1006127516791.

Kleinhentz, M., Jactel, H., Menassieu, P., 1999. Terpene attractant candidates of Dioryctria sylvestrella in maritime pine (Pinus pinaster) oleoresin, needles, liber, and headspace samples. J. Chem. Ecol. 25, 2741–2756. https://doi.org/10.1023/A:1020803608406.

Kourtchev, I., Godoi, R.H.M., Connors, S., Levine, J.G., Archibald, A.T., Godoi, A.F.L., Paralovo, S.L., Barbosa, C.G.G., Souza, R.A.F., Manzi, A.O., Seco, R., Sjostedt, S., Park, J.-H., Guenther, A., Kim, S., Smith, J., Martin, S.T., Kalberer, M., 2016. Molecular composition of organic aerosols in central Amazonia: an ultra-high-resolution mass spectrometry study. Atmos. Chem. Phys. 16, 11899–11913. https://doi.org/10.5194/acp-16-11899-2016.

Laothawornkitkul, J., Taylor, J.E., Paul, N.D., Hewitt, C.N., 2009. Biogenic volatile organic compounds in the earth system. New Phytol. 183, 27–51. https://doi.org/10.1111/j.1469-8137.2009.02859.x.

Lelieveld, J., Butler, T.M., Crowley, J.N., Dillon, T.J., Fischer, H., Ganzeveld, L., Harder, H., Lawrence, M.G., Martinez, M., Taraborrelli, D., Williams, J., 2008. Atmospheric oxidation capacity sustained by a tropical forest. Nature 452, 737. https://doi.org/10.1038/nature06870.

Li, H., Canagaratna, M.R., Riva, M., Rantala, P., Zhang, Y., Thomas, S., Heikkinen, L., Flaud, P.-M., Villenave, E., Perraudin, E., Worsnop, D., Kulmala, M., Ehn, M., Bianchi, F., 2020a. Source identification of atmospheric organic vapors in two European pine forests: results from Vocus PTR-TOF observations. Atmos. Chem. Phys. 20, 648. https://doi.org/10.5194/acp-2020-648.

Li, H., Riva, M., Rantala, P., Heikkinen, L., Daellenbach, K., Krechmer, J.E., Flaud, P.-M., Worsnop, D., Kulmala, M., Villenave, E., Perraudin, E., Ehn, M., Bianchi, F., 2020b. Terpenes and their oxidation products in the French Landes forest: insights from Vocus PTR-TOF measurements. Atmos. Chem. Phys. 20, 1941–1959. https://doi.org/10.5194/acp-20-1941-2020.

Liebmann, J., Sobanski, N., Schuladen, J., Karu, E., Hellén, H., Hakola, H., Zha, Q., Ehn, M., Riva, M., Heikkinen, L., Williams, J., Fischer, H., Lelieveld, J., Crowley, J.N., 2019. Alkyl nitrates in the boreal forest: formation via the NO_3-, OH- and O_3-induced oxidation of biogenic volatile organic compounds and ambient lifetimes. Atmos. Chem. Phys. 19, 10391–10403. https://doi.org/10.5194/acp-19-10391-2019.

Lou, S., Holland, F., Rohrer, F., Lu, K., Bohn, B., Brauers, T., Chang, C.C., Fuchs, H., Häseler, R., Kita, K., Kondo, Y., Li, X., Shao, M., Zeng, L., Wahner, A., Zhang, Y., Wang, W., Hofzumahaus, A., 2010. Atmospheric OH reactivities in the Pearl River Delta – China in summer 2006: measurement and model results. Atmos. Chem. Phys. 10, 11243–11260. https://doi.org/10.5194/acp-10-11243-2010.

Mao, J., Ren, X., Zhang, L., Van Duin, D.M., Cohen, R.C., Park, J.-H., Goldstein, A.H., Paulot, F., Beaver, M.R., Crounse, J.D., Wennberg, P.O., DiGangi, J.P., Henry, S.B., Keutsch, F.N., Park, C., Schade, G.W., Wolfe, G.M., Thornton, J.A., Brune, W.H., 2012. Insights into hydroxyl measurements and atmospheric oxidation in a California forest. Atmos. Chem. Phys. 12, 8009–8020. https://doi.org/10.5194/acp-12-8009-2012.

Mermet, K., Sauvage, S., Dusanter, S., Salameh, T., Léonardis, T., Flaud, P.-M., Perraudin, E., Villenave, E., Locoge, N., 2019. Optimization of a gas chromatographic unit for measuring BVOCs in ambient air. Atmos. Meas. Tech. 12, 6153–6171. https://doi.org/10.5194/amt-12-6153-2019.

Mogensen, D., Gierens, R., Crowley, J.N., Keronen, P., Smolander, S., Sogachev, A., Nölscher, A.C., Zhou, L., Kulmala, M., Tang, M.J., Williams, J., Boy, M., 2015. Simulations of atmospheric OH, O_3 and NO_3 reactivities within and above the boreal forest. Atmos. Chem. Phys. 15, 3909–3932. https://doi.org/10.5194/acp-15-3909-2015.

Moreaux, V., Lamaud, É., Bosc, A., Bonnefond, J.-M., Medlyn, B.E., Loustau, D., 2011. Paired comparison of water, energy and carbon exchanges over two young maritime pine stands (Pinus pinaster Ait.): effects of thinning and weeding in the early stage of tree growth. Tree Physiol. 31, 903–921. https://doi.org/10.1093/treephys/tpr048.

Nagnan, P., Clement, J.L., 1990. Terpenes from the maritime pine Pinus pinaster: toxins for subterranean termites of the genus Reticulitermes (Isoptera: Rhinotermitidae)? Biochem. Syst. Ecol. 18, 13–16. https://doi.org/10.1016/0305-1978(90)90025-B.

Niinemets, Ü., Arneth, A., Kuhn, U., Monson, R.K., Peñuelas, J., Staudt, M., 2010. The emission factor of volatile isoprenoids: stress, acclimation, and developmental responses. Biogeosciences 7, 2203–2223. https://doi.org/10.5194/bg-7-2203-2010.

Nölscher, A.C., Williams, J., Sinha, V., Custer, T., Song, W., Johnson, A.M., Axinte, R., Bozem, H., Fischer, H., Pouvesle, N., Phillips, G., Crowley, J.N., Rantala, P., Rinne, J., Kulmala, M., Gonzales, D., Valverde-Canossa, J., Vogel, A., Hoffmann, T., Ouwersloot, H.G., Vilà-Guerau de Arellano, J., Lelieveld, J., 2012. Summertime total OH reactivity measurements from boreal forest during HUMPPA-COPEC 2010. Atmos. Chem. Phys. 12, 8257–8270. https://doi.org/10.5194/acp-12-8257-2012.

Peräkylä, O., Vogt, M., Tikkanen, O.-P., Laurila, T., Kajos, M.K., Rantala, P.A., Patokoski, J., Aalto, J., Yli-Juuti, T., Ehn, M., Sipilä, M., Paasonen, P., Rissanen, M., Nieminen, T., Taipale, R., Keronen, P., Lappalainen, H.K., Ruuskanen, T.M., Rinne, J., Kerminen, V.-M., Kulmala, M., Bäck, J., Petäjä, T., 2014. Monoterpenes' oxidation capacity and rate over a boreal forest: temporal variation and connection to growth of newly formed particles. Boreal Environ. Res. 19, 293–310.

Petäjä, T., Mauldin, I.I.I., Kosciuch, E., McGrath, J., Nieminen, T., Paasonen, P., Boy, M., Adamov, A., Kotiaho, T., Kulmala, M., 2009. Sulfuric acid and OH concentrations in a boreal forest site. Atmos. Chem. Phys. 9, 7435–7448. https://doi.org/10.5194/acp-9-7435-2009.

Petersson, G., 1988. High ambient concentrations of monoterpenes in a scandinavian pine forest. Atmos. Environ. 22, 2617–2619. https://doi.org/10.1016/0004-6981(88)90497-0.

Plewka, A., Gnauk, T., Brüggemann, E., Herrmann, H., 2006. Biogenic contributions to the chemical composition of airborne particles in a coniferous forest in Germany. Atmos. Environ. 40, 103–115. https://doi.org/10.1016/j.atmosenv.2005.09.090 Regional biogenic emissions of reactive volatile organic compounds (BVOC) from forests: Process studies, modelling and validation experiments (BEWA2000).

Simon, V., Clement, B., Riba, M.-L., Torres, L., 1994. The Landes experiment: Monoterpenes emitted from the maritime pine. J. Geophys. Res. Atmospheres 99, 16501–16510. https://doi.org/10.1029/94JD00785.

Sinha, V., Williams, J., Lelieveld, J., Ruuskanen, T.M., Kajos, M.K., Patokoski, J., Hellen, H., Hakola, H., Mogensen, D., Boy, M., Rinne, J., Kulmala, M., 2010. OH reactivity measurements within a boreal forest: evidence for unknown reactive emissions. Environ. Sci. Technol. 44, 6614–6620. https://doi.org/10.1021/es101780b.

Stocker, T.F., Qin, D., Plattner, G.-K., Tignor, M., Allen, S.K., Boschung, J., Naeuls, A., Xia, Y., Bex, V., Midgley, P.M., 2013. IPCC, 2013: Climate Change 2013: The Physical Science Basis. Contribution of Working Group I to the Fifth Assessment Report of the Intergovernmental Panel on Climate Change, Cambridge University Press, Cambridge. IPPC, United Kingdom and New York, NY, USA.

Taraborrelli, D., Lawrence, M.G., Crowley, J.N., Dillon, T.J., Gromov, S., Groß, C.B.M., Vereecken, L., Lelieveld, J., 2012. Hydroxyl radical buffered by isoprene oxidation over tropical forests. Nat. Geosci. 5, 190–193. https://doi.org/10.1038/ngeo1405.

Taylor, B.N., Kuyatt, C.E., 1994. NIST technical note 1297. Edition. Guidelines for Evaluating and Expressing the Uncertainty of NIST Measurement Results.

Villena, G., Bejan, R., Kurtenbach, R., Wiesen, P., Kleffmann, J., 2012. Interferences of commercial NO_2 instruments in the urban atmosphere and in a smog chamber. Atmos. Meas. Tech 5, 149–159. https://doi.org/10.5194/amt-5-149-2012.

Vrekoussis, M., Kanakidou, M., Mihalopoulos, N., Crutzen, P.J., Lelieveld, J., Perner, D., Berresheim, H., Baboukas, E., 2004. Role of the NO_3 radicals in oxidation processes in the eastern Mediterranean troposphere during the MINOS campaign. Atmospheric Chem. Phys 4, 169–182. https://doi.org/10.5194/acp-4-169-2004.

Wolfe, G.M., Cantrell, C., Kim, S., Mauldin III, R.L., Karl, T., Harley, P., Turnipseed, A., Zheng, W., Flocke, F., Apel, E.C., Hornbrook, R.S., Hall, S.R., Ullmann, K., Henry, S.B., DiGangi, J.P., Boyle, E.S., Kaser, L., Schnitzhofer, R., Hansel, A., Graus, M., Nakashima, Y., Kajii, Y., Guenther, A., Keutsch, F.N., 2014. Missing peroxy radical sources within a summertime ponderosa pine forest. Atmos. Chem. Phys. 14, 4715–4732. https://doi.org/10.5194/acp-14-4715-2014.

Yáñez-Serrano, A.M., Nölscher, A.C., Bourtsoukidis, E., Gomes Alves, E., Ganzeveld, L., Bonn, B., Wolff, S., Sa, M., Yamasoe, M., Williams, J., Andreae, M.O., Kesselmeier, J., 2018. Monoterpene chemical speciation in a tropical rainforest:variation with season, height, and time of dayat the Amazon Tall Tower Observatory (ATTO). Atmos. Chem. Phys. 18, 3403–3418. https://doi.org/10.5194/acp-18-3403-2018.

Yassaa, N., Song, W., Lelieveld, J., Vanhatalo, A., Bäck, J., Williams, J., 2012. Diel cycles of isoprenoids in the emissions of Norway spruce, four Scots pine chemotypes and in Boreal forest ambient air during HUMPP-COPEC-2010. Atmos. Chem. Phys. 12, 7215–7229. https://doi.org/10.5194/acp-12-7215-2012.

Zannoni, N., Gros, V., Sarda Esteve, R., Kalogridis, C., Michoud, V., Dusanter, S., Sauvage, S., Locoge, N., Colomb, A., Bonsang, B., 2017. Summertime OH reactivity from a receptor coastal site in the Mediterranean Basin. Atmos. Chem. Phys. 17, 12645–12658. https://doi.org/10.5194/acp-17-12645-2017.